U. of Iowa 68-26

Energetic Particles in the Outer Magnetosphere: Explorer 33*

by

G. P. Haskell

Department of Physics and Astronomy
University of Iowa
Iowa City, Iowa 52240

March 1968

*This work was supported in part by National Aeronautics and Space Administration Grant ~~NsG 233-62~~ and Goddard Space Flight Center/ National Aeronautics and Space Administration Contract NAS 5-9076.

NSL-16-001-002

ABSTRACT

The fluxes of energetic particles (electrons, $E \geq 45$ keV; protons, $E \geq 730$ keV) seen between about 5 and 20 earth radii from the earth by Explorer 33 are examined. It is shown that most of the features seen in the time profiles of the flux can be attributed to a single, spatially-continuous central body of trapped particles whose boundary is everywhere oscillating in position. Even very strong variations in the flux, including "detached spikes" at the sunward boundary, can be attributed to these oscillations. The flux in the outer regions of this body is usually anisotropic. On the day side the flux is peaked at right angles to the local magnetic field whereas on the night side it is peaked along the field. Two exceptions to this rule were found. These observations are compared with previous ones and are discussed in the light of current theory.

I. INTRODUCTION

Energetic particles in the outer regions of the earth's magnetosphere have been studied for several years in the hope of gaining a greater understanding of the physical processes that lead to phenomena such as auroras and magnetic storms. It is now generally believed that these diverse magnetospheric phenomena result basically from the interaction of the solar wind with the earth's magnetic field. However, the details of the mechanisms involved are poorly understood.

A study of energetic particles using Explorer 33 might be expected to shed new light on problems of magnetospheric physics for two main reasons. First, the trajectory of this satellite takes the detectors along paths through the magnetosphere which have not been traversed before. For example, on certain orbits the satellite skims slowly past the magnetosphere near its outer boundary on the sunward side. Second, the detectors on this spinning satellite are "sectored" so that we have information about the anisotropy of the particle fluxes. This is a factor which has received little study in the outer magnetosphere.

These two features enable us to look at the magnetosphere in a slightly different way. Some important previous observations,

which form the background for this study, are outlined in the following paragraphs.

The first comprehensive survey of energetic particles (electrons, $E \geq 40$ keV) in the outer magnetosphere was made by Frank [1965] using Explorer 14. The principal conclusions were as follows: (1) There is a "core" in which high fluxes are always found. This extends as far as 8 R_E near the magnetic equatorial plane and has a weak latitude dependence. (2) Beyond the core there are severe variations in flux between one pass and another. (3) The radial extent of the region in which fluxes $\geq 10^5$ cm^{-2} sec^{-1} are found increases from about 11 R_E near local noon to ≥ 16 R_E near local morning and evening. (4) There is a "tail" of electrons beyond about 10 R_E on the night side confined near the ecliptic plane and extending at least to the satellite apogee at about 16 R_E.

Anderson [1965], in a paper devoted mainly to a study of particle fluxes at greater distances (up to 31.5 R_E), described the observations made by IMP 1 of the energetic particles surrounding the earth. His findings were as follows. (1) The stably trapped particles exhibit a smooth profile. (2) Beyond this region is a "skirt" in which fluctuations in the profile are seen. This skirt extends toward the noon meridian, and perhaps across it, and as far as a sun-earth-probe angle of 120° or 130°. (3) At

larger angles, characteristic fast-rise, slow-fall fluctuations are seen. This region, which is called the "cusp", extends across the midnight meridian; it is confined in latitude and ends abruptly between 10 and 15 R_E. This is identified with the tail described by Frank. Anderson and Ness [1966] showed that, on most occasions, the magnetic field is depressed in the particle cusp region. (4) Outside these regions, isolated "islands" of flux are seen. These also exhibit the fast-slow behavior.

The extent of the trapping region for electrons, E ~ 100 keV, was shown by Serlemitsos [1966] to be variable in time, extending as far as 12 R_E near midnight at low latitudes on magnetically quiet days. He also showed that the intensities are peaked along the magnetic field direction in the distant regions instead of perpendicular to it as in the regions closer to the earth. Rothwell [1967] has shown that the distant trapping zone extends out to 12 to 16 R_E on the dark side of the earth. Anderson et al. [1965] report that near dawn 40 keV electron fluxes are seen beyond the magnetopause and even beyond the bow shock as defined magnetically. At the particle boundary near local noon, spikes of electrons separated from the main body of particles have been described by many authors including Rosser [1963], Frank and Van Allen [1964], Frank [1965], Anderson et al. [1965], and Fan et al. [1964 and 1965].

Using the Vela satellites, which have nearly circular orbits at about 17 R_E, Bame et al. [1967] obtained the following results. (1) The 40 keV fluxes are part of the high energy tail of the energy distribution. The variations in the 40 keV fluxes are associated with variations in the average energy (temperature) of the plasma. (2) This plasma forms a sheet which is about 4 to 6 R_E thick near midnight and flares to about twice this thickness near local dawn and dusk. (3) The center of the sheet lies between the solar magnetospheric and geomagnetic equators. (4) There is a strong asymmetry between the dawn and dusk sides of the magnetosphere in that energetic electrons are seen much more frequently on the dawn side.

More recently, Montgomery [1968] has shown that sometimes the energetic electrons do not form a smooth high energy tail to the energy distribution, but are part of a separate energy distribution with a secondary flux maximum at about 10 keV.

Periodic modulations of the flux of energetic particles have been observed. Judge and Coleman [1962] observed periods of 100 to 500 seconds in the modulations of flux and magnetic field in the outer zone. Lin and Anderson [1966] report that periodic modulations are seen throughout the distant radiation zone--even out to $\sim$ 30 R_E in the tail. The periods tend to be close to six

minutes. These modulations are interpreted as a manifestation of hydromagnetic waves.

Some detailed results from the papers quoted above, and from some other papers, are compared with the results of this study in the discussion section.

II. EXPERIMENTAL DETAILS

Explorer 33 was launched on 1 July 1966 into a very eccentric orbit about the earth with an apogee at about 80 R_E and a period of about 17 days. The perigee varies from about 5 to 15 R_E, and it is this near-perigee part of the orbit that we are concerned with here. Figure 1 shows, in geocentric solar ecliptic coordinates, those segments of the first 17 orbits that are used in this study. The passes are numbered chronologically to help in locating the matching pairs of curves in the two projections. The numbers are placed at the beginning of each segment of orbit.

The satellite was spin-stabilized during the launching operation with its axis near the ecliptic plane. Thereafter, the spin axis remained approximately fixed in celestial coordinates, which means that it moved through roughly one degree per day in solar ecliptic coordinates.

The detectors that provided the data for this study were the Geiger-Müller tubes in the University of Iowa's experiment [Van Allen and Ness, 1967]. There were three EON 6213 mica-window tubes. Two, labelled GM2 and GM3, pointed in opposite directions along the satellite's spin axis and had conical collimators. The other, GM1, pointed at right angles to the spin axis and had a fan-shaped

collimator. Details are given in Figure 2. The energy thresholds of GM1 were about 50 keV for electrons and 830 keV for protons. The thresholds for GM2 and GM3 were about 45 keV and 730 keV for electrons and protons, respectively. The slight difference in energy threshold between the detectors has been ignored, and no attempt has been made to distinguish between electrons and protons.

The output of GM1 was sorted into four storage registers according to which of the four quadrants shown in Figure 2 contained the axis of the collimator. The electronic generation of the sectors was triggered by a "see-sun" pulse from a narrow angle photoelectric sensor. The spin period was about 2.3 seconds and the output of each detector was accumulated for 25.57 seconds. Thus, the storage time for each sector was 6.39 seconds. The output from each sector was transmitted from the satellite once per telemetry sequence (81.808 seconds). The outputs from GM2 and GM3 were transmitted once in every two sequences.

III. RESULTS

We must first discuss our choice of coordinate systems. No single set of coordinates can be expected to organize the data adequately over the whole region to be studied here. Solar ecliptic coordinates should be the best in the most distant magnetosphere where the influence of the solar wind is strong. See, for example, Frank [1965]. Geomagnetic coordinates should be best closer to the earth where the earth's dipole field dominates. Solar magnetospheric coordinates, as a compromise between the two previously mentioned systems, have been only partially successful in organizing the data. See Bame et al. [1967]. For the present study, we have taken geocentric solar ecliptic coordinates for the basic frame of reference and taken account of the geomagnetic latitude whenever it was thought to be important. We have also made use of simultaneous measurements of the local magnetic field to locate the position of the satellite with respect to boundaries, such as the magnetopause and the neutral sheet.

The basic results are contained in Figure 3 which shows the counting rate profiles, together with Figure 1 which displays the trajectory of the satellite. The diamond-shaped symbols which appear on both sets of figures enable the positions of the particle

fluxes to be determined. The background due to cosmic rays is usually less than one count per second. It is sometimes much greater because of the presence of solar particles.

The quantities GA, GB, and GC plotted in Figure 3 are defined as follows. GA is the average of the counting rates of Sectors I and III of GM1, GB is the average of Sectors II and IV, and GC is the average of GM2 and GM3, except for the following modifications. During days 282 to 334, GM2 was directed toward the sun and responded to solar x-rays. The x-rays dominated the response and therefore GM2 was eliminated from the average. Thus, GC represents the counting rate of GM3 alone during this period. For the remainder of the period of this investigation, Sector III detected solar x-rays and was eliminated from GA which, therefore, then represents the counting rate of Sector I only. The counting rates have been reduced to counts per second and the three quantities have been normalized so that in a completely isotropic flux, GA, GB, and GC are identical. This normalization was necessary because of the slightly different geometric factors. The flux in particles cm^{-2} $sterad^{-1}$ sec^{-1} is obtained by multiplying the counting rate per second by approximately 40.

GA, GB, and GC are intended to represent the particle flux in three mutually orthogonal directions and, therefore, to give

an indication of anisotropy. These quantities are meaningful only if Sectors I and III, II and IV, and GM2 and GM3, respectively, detect nearly identical fluxes, i.e., if there is no net flow of particles. This condition was nearly always fulfilled. The exceptions are important and are discussed separately.

We shall now proceed to examine the counting rate profiles, restricting ourselves in this section to a phenomenological description of their main features and a concise account of some of the most immediate inferences. We leave the discussion of the significance of the observations and comparison with other measurements until the next section.

A. The Central Body of Particles

A brief perusal of the profiles suggests that there is, as expected, a central body of trapped particles. We examine first the extent of this region.

1. Boundary

Moving outward from the region of high flux in the profiles, it is always possible (except where there are data gaps) to locate a point at which the flux first drops to background. The positions thus identified are all marked with a black diamond. Their locations on the orbits are similarly marked on Figure 1. We see that,

except near the noon meridian, the extent of this region is quite variable, ranging from about 7 R_E on orbit 15 to about 16 R_E on orbit 3.

Most of this variation can be eliminated, at least on the dusk (+Y) side, by taking account of the geomagnetic latitude of the points. On the first ten orbits and orbit 13, the trajectory of the satellite was such that the boundary was always crossed at very low geomagnetic latitudes. Almost all of these crossings were within 10° of the geomagnetic equator. On orbits 11, 12, 14, and 15 the satellite crossed the boundary at relatively high latitudes, thus giving a false impression of the radial extent of the central body of particles.

In Figure 4, we show the trajectory of orbit 12 in geomagnetic coordinates--radial distances versus geomagnetic latitude, ignoring longitude. The two patches of particles seen in the time profile are then very simply explained as two encounters with a single body of particles confined within a region such as the one suggested by the dashed line. The satellite briefly energes from the particle region between the time of the second diamond and the short data gap.

The profiles from the other passes can be interpreted in a similar way, and the positions of the boundary as defined by these passes are also marked on Figure 4. The remaining scatter in the

points can be plausibly attributed to relatively minor variations, with longitude and time, of the size and shape of the "lobe" sketched by the dashed line. The main inference is that on all the passes through the dusk side of the magnetosphere, this lobe was filled with trapped energetic particles. That the particles are trapped is inferred from the relative smoothness of the profiles and the anisotropy.

2. Anisotropy

An important feature in the central body of particles is the anisotropy which is seen near the boundary on most passes, and which decreases or disappears as the satellite moves further into the region. On the "night" side, the flux is usually peaked along the field direction. On the "day" side, it is not peaked along the field but appears to be peaked at right angles to it. To demonstrate this effect, we present Figure 5. Our aim is to compare the direction of the field vector with the direction of maximum particle flux. If these two are identical, we expect points to lie on the solid line. If they differ by 90°, we expect them to lie on the dashed lines.

Figure 5 was constructed by the following procedure. We consider only components of field and particle flux perpendicular to the satellite spin axis. Some information is wasted this way,

but the analysis is greatly simplified and the results are adequate for present purposes. The field direction was obtained by projecting the satellite-sun line and the field vector onto a plane at right angles to the spin axis. The field direction is the angle between these projections, counted positive from the projection of the satellite-sun line in the direction of rotation of the satellite. Since a field at A° has the same effect on trapped particles as a field at A° + 180°, we subtract 180° from angles that exceed 180°.

To find the exact direction of maximum flux, one needs to know the distribution of pitch angles and to combine this with the angular acceptance of the collimators. Since the pitch angle distribution is unknown and since there is no physical basis for choosing any particular analytical form, we can only hope to assign an approximate value to the direction of maximum flux. We calculate simply the angle $\tan^{-1}$ (GA/GB) and say that the direction of maximum flux, in the plane perpendicular to the spin axis, is approximately $\alpha = 85° \pm \tan^{-1}$ (GA/GB). The origin of the 85° can be seen in Figure 2. There is an inherent ambiguity about which quadrant the angle should be in (whether to use the plus or the minus sign). The quadrant was chosen by the following procedure. The series of points for each pass was produced by calculating the field direction and α once every ten sequences in the region of interest. Then,

whenever possible, the quadrant was chosen so that α and the field direction bore a constant relationship, i.e., so that the series of points lay roughly parallel to the lines marked on the figure.

The result is that points from the day and night sides are clearly separated. The night side flux is shown to be peaked along the field; the day side flux is shown not to be peaked along the field. It is likely that this flux is peaked at right angles to the field, but that our approximation is not good enough to show this accurately.

The measurements made on orbits 11 and 12 have been omitted from Figure 5 and are shown separately on Figure 6. The relationship between α and the field direction suddenly changes and subsequent points, which are shown joined, move further from the solid line and toward the dashed line. It appears that the pitch angle distribution changes from one in which the flux is peaked along the field to one in which the flux is peaked at right angles to the field. Whether this is a spatial or temporal change, it is, of course, impossible to know. A possible clue to the cause of the change is furnished by the magnetic field measurements. Just as α starts to change appreciably from the field direction, the magnitude of the field starts to increase more rapidly than before. This is shown in Figure 7.

3. Oscillations and Spikes

Just inside the particle boundary, modulations in the intensity of the particle flux are seen on every occasion. The modulations are roughly periodic with a period of a few minutes, typically ten minutes, and we therefore refer to them as oscillations. Orbits 9 and 10 provide examples of large amplitude oscillations; orbit 3 shows oscillations of smaller amplitude which are sustained for seven hours.

The oscillations seen on orbits 2 and 9, near the sunward boundary, are worthy of further examination because they are followed (or preceded) by "detached spikes" of particles. Taking orbit 9 (Figure 8), we first note that the profile of the spikes is very similar to the profile of the oscillations. Further, we note that the anisotropy seen in the spikes is the same as that which is seen in the oscillations and in the more stable flux behind. This strongly suggests that the particles seen in the spikes are part of the central body of particles, and that the spikes are caused by the particle boundary moving back and forth across the satellite.

Simultaneous measurements of the magnetic field support this view. The sequence-averaged vector field measurements from the Ames magnetometer are plotted in Figure 8. From a study of

all the magnetopause crossings on the sunward side, it is clear that the magnetopause crossing is marked by a change in the direction of the field vector from one fairly steady value within the magnetosphere to a different, but still fairly steady, value in the magnetosheath (or transition region). Sometimes the field switches back and forth between the two directions before finally settling down. The magnetopause crossing on orbit 9 is a good example of the latter type. The important fact is that the peak particle fluxes occur when the field switches back to the direction it had inside the magnetosphere. It is difficult to avoid the conclusion that a boundary is moving back and forth across the satellite.

The changes in the magnitude of the field can be understood qualitatively in terms of a moving boundary. Within the region of oscillations, the dips in the particle intensity are accompanied by increases in the field strength. This is consistent with compression of the magnetosphere at these times. The spikes are accompanied by a decrease in the field strength. This is consistent with an expansion of the magnetosphere.

The position of the magnetopause, as determined by the magnetic measurements alone, is marked by a bar on the time profiles. The length of the bar shows the time that elapsed between the first

departure from one steady field direction and the final attainment of the other. This determination is sometimes rather subjective.

The other occasion on which detached spikes were seen (out of six passes through the magnetopause within 60° of the sub-solar point) is on orbit 2, which is displayed in Figure 9. These spikes cannot be explained in exactly the same way as the spikes on orbit 9, but we reach the same final conclusion, namely that they are most simply explained as the result of a moving boundary.

In this case, although the profiles of the spikes and the oscillations are similar, we cannot say that the anisotropy is the same in the spikes, the oscillations, and the inner region. The field direction, although it changes slightly during the spikes, does not change to the value characteristic of the magnetosphere. The important clue in this case is that the particles in the spikes are streaming. Our quantities GA, GB, and GC are therefore meaningless and we plot instead, on Figure 9, GM2 and GM3, the two detectors that point in opposite directions along the spin axis. In Figure 8, we plotted two sectors that pointed in perpendicular directions. This figure shows that streaming particles are also seen in the outer part of the region of oscillations. These fluxes of streaming particles are encountered while the field still has its transition region value and just before it changes to its

magnetosphere value. It therefore seems likely that the streaming particles are characteristic of the part of the transition region that is adjacent to the magnetopause. The spikes and the associated small field changes are then easily explained. They are due to a boundary movement in which the magnetopause does not quite reach the incoming satellite, but reaches far enough so that the satellite is immersed in the streaming particles just beyond the magnetopause.

Figure 10 shows the simplest crossing of the magnetopause (from orbit 12) on an expanded scale. The small peaks of streaming particles are just beyond the magnetopause as defined magnetically by our criterion, which tends to confirm our inference that streaming particles are characteristic of this region.

In Figure 8, in addition to the major modulations of the flux which we have accounted for, there are small peaks near the outer edge in which Sector II exceeds Sector I, which we have not accounted for. The output of the other sectors shows that the particles are streaming at these points. Since these particles are just beyond the magnetopause as defined by the magnetic field, we believe that they too are transition region particles of the same sort as those seen in Figures 9 and 10.

Orbit 5 is relevant at this point. This is an orbit which skims very near the magnetopause on the day side. The anisotropy

of the particle fluxes that are encountered is evidence that they are of the same kind as those normally seen just inside the particle boundary. The simplest explanation of the fluctuations--of up to three orders of magnitude, seen over a period of 24 hours--is that the boundary is moving back and forth, i.e., oscillating, near the satellite.

In addition to showing boundary oscillations with a period of a few minutes, this profile seems to reveal superimposed oscillations with a period of about 2.2 hours, there being six cycles between the diamond symbols.

We tentatively interpret the profile of orbit 6 as additional evidence of boundary movements. Because of the lack of any smooth profile or sustained anisotropy, we cannot positively identify the particles as trapped particles, but the location of the trajectory and the great intensity of the flux argue in favor of this interpretation. The flux often increases within a few minutes and then decreases in about two hours with oscillations of a few minutes superimposed on the decreasing part. This implies rapid expansions of the particle region followed by slower contractions. During this pass, the magnetic activity at the earth, as determined by K_p indices, was greater than on any other pass.

B. Particles Beyond the Central Body

In the previous section, the inference has been drawn that many of the patches of particle flux that are detached from the central body of particles in the time profile are, in fact, part of that single, spatially-continuous central body of particles. There remain some patches which have not been accounted for. These are seen on orbits 7 to 9 and 16. They occur on the dawn (-Y) side of the magnetosphere and near the midnight meridian. We shall deal with each region separately.

1. On the Dawn Side

The particles seen on orbits 7 and 8, unlike those on the dusk side, cannot be positively identified as trapped particles. The profiles are nowhere smooth and no sustained anisotropy is seen. The profiles are best described as "spiky".

The dawn side is sampled much less evenly by the satellite than the dusk side. Orbits 7 and 8 are within 20° of the magnetic equator most of the time, but orbits 15 and 16 pass at high magnetic latitudes. On orbits 7 and 8, the profiles are not unlike those seen at the extreme edge of the particle region on the dusk side, and it is therefore possible that the orbits pass near the boundary of a large body of trapped particles on the dawn side. However, the local magnetic field, like the profiles, was much more

erratic during these passes than during passes through the dusk side. The fluctuations were such that we were unable to locate the magnetopause on these passes.

2. Near Midnight

Orbits 9, 10, and 16 cross the midnight meridian at distances of about 12.5, 10, and 9 R_E, respectively, and might be expected to yield information about the region of transition from the tail-like field to the dipole-like field.

As shown in Figure 11, it is quite reasonable to suppose that the patches on orbits 9 and 16 are confined near the surface formed by the geomagnetic equator and a neutral sheet, parallel to the X axis, which joins the equator at about 8.5 and 12 R_E, respectively.

This supposition is fully confirmed by the simultaneous magnetic field measurements, which provide a much more accurate frame of reference than the dashed lines on Figure 11. On orbit 16, a clearly defined, neutral sheet crossing occurs during the particle observation. This is shown in Figure 12. On orbit 10, the field changes from a tail-like field directed away from the sun to a dipole-like field. The change starts abruptly, just as the anisotropic flux is encountered, with a sharp decrease in field strength. The patch of particles on orbit 9 coincides with a region

of depressed field strength in which the direction of the field changes slowly from anti-solar to the reverse, as shown in Figure 13. This is like an expanded neutral sheet crossing. After an abrupt increase in the field strength, which coincides exactly with the flux decrease marked by a black diamond, the field starts to look like a dipole field.

To aid in visualizing these configurations, we present Figure 14. This is an idealized sketch of a plausible field configuration in which the neutral sheet and magnetic equator have been "bent" to form a straight line. The orbits in this frame of reference (which is the only important frame of reference) are approximately as shown. This figure suggests than even the "tail" of particles seen here should more properly be considered part of the central body of particles, the boundary of the particle region being determined by the field lines which are very distorted, but still continuous in this region.

A high degree of anisotropy is seen on orbit 9. Once again, as demonstrated in Figure 15, the flux is peaked <u>along</u> the field lines.

IV. DISCUSSION

A general conclusion that can be reached from the foregoing results is that a large number of the features seen in the time profiles can be attributed to a single, continuous central body of trapped particles, whose boundary is everywhere oscillating in position. In this interpretation, the large patches on the dawn side result from multiple intersections of the trajectory with the particle region; the detached spikes on the sunward side result from rapid movements of the particle boundary past the relatively slowly moving satellite; the midnight tail of particles near the neutral sheet is the extension of the particle region into the drawn out field; the very large and sustained fluctuations (e.g., orbits 5 and 11) are due to movements of the particle boundary while the satellite is passing close to and nearly parallel to the boundary; the oscillation of the intensity of the flux within the particle region results directly from the oscillatory movement of the boundary.

This interpretation has the virtue of economy, and moreover, is able to give a simple explanation of some very strong fluctuations (e.g., orbit 11) of the kind that have previously defied explanation.

The precise shape of this central body of particles is not defined by the small number of measurements made here. They show only that the meridional cross section must be a function of longitude. The more extensive measurements made by Rothwell [1967] give a clearer picture of the shape of the region. The boundary of the "distant radiation zone" as defined by Rothwell is the same as the boundary of the central body of particles defined here. Figure 16 shows, qualitatively, the kind of variation of cross section with longitude that is needed to fit the present observations.

The particles that yield the spiky profiles on the dawn side cannot be positively identified as part of this central body of particles. They could be part of the extreme outer edge of this body, but the fact that the magnetic field is more disturbed suggests that they cannot be explained so simply. In this context, it may be significant that an asymmetry between the dawn and dusk sides of the magnetosphere has been reported by other authors. Bame et al. [1967] showed that 40 keV electrons are seen at $\sim$ 17 R_E much more frequently on the dawn side. The present results are consistent with this. On the dusk side, the particle fluxes often terminate closer than 17 R_E, whereas the spiky profiles on the dawn side extend to beyond 17 R_E. The extensive magnetic

observations of Heppner et al. [1967] also suggest an asymmetry. They too had difficulty in locating the magnetopause near the dawn meridian at low latitudes. They found that the average field gradient beyond 11 R_E in this region was nearly zero, and they show that β (the ratio of the plasma pressure to the magnetic pressure) was probably near to or greater than unity. They speculate that this could result in solar wind plasma being able to enter the magnetosphere in this region, either continuously or intermittently. From a lack of similar observations on the dusk side, they conclude that this region of high β may be limited to a narrower range of latitudes if it exists as a persistent feature on this side. Since the coverage of the midnight-to-dawn quadrant by Explorer 33 was poor, we do not have enough information to be able to speculate further about the cause of these spiky profiles.

We have chosen to describe our inferred particle distributions mostly by new and fairly neutral phrases. The terms used by previous authors have usually been given precise definitions, which prevent them from adequately describing the present observations. For instance, the core defined by Frank [1967] bears little relationship to our central body of particles. The method of analysis used by Frank emphasized fluctuations in

intensity between one pass and another at given values of L. The core then assumes a statistical nature. It is the L-shell within which the intensity is always high ($\gtrsim 10^7$ cm^{-2} sec^{-1}). In the present study, the absolute value of the flux is of minor importance. The tail of particle flux observed by Frank is presumably the same as the tail, confined near the neutral sheet, that we observe. This tail is also presumably related to the particle cusp described by Anderson [1965]. However, we do not see in the tail the fast-rise, slow-fall fluctuations which Anderson used to distinguish the cusp region from other regions. The only fast-slow fluctuations that we see are in the high latitude parts of orbit 16 and in orbit 6. In orbit 6, the satellite is in the region that is called the skirt by Anderson, and which is characterized in his scheme by the absence of fast-slow fluctuations.

The distribution of particles has been inferred from satellite trajectories which, in some regions, sample the magnetosphere in a very exacting way. For instance, orbits 1 to 3 and 12 to 15 are roughly orthogonal on the dusk side. However, the total number of passes is small and it is possible that the observed fluxes were not typical. It is clear that further study is required.

B. Oscillations and Spikes

The periodic modulations in the flux are similar to those seen by Judge and Coleman [1962], Lin and Anderson [1966], and Anderson et al. [1968]. The new feature seen here is that these oscillations are characteristic of the entire outer edge of the central body of particles.

The flux oscillations require merely a smooth spatial gradient in the flux near the boundary and an oscillatory movement of this boundary region at right angles to the gradient. The situation is almost certainly complicated by simultaneous changes in the field strength which change the energy of the particles and thereby change the flux detected by the threshold counters. That is to say, a hydromagnetic description is called for.

The precise point at which the flux oscillations cease, moving inward, is probably relatively unimportant. There is no reason why the hydromagnetic disturbance should not continue to propagate after it has ceased to manifest itself by significantly modulating the high energy flux. The severity of the modulation of the high energy flux by a given disturbance depends on the spatial flux gradient, the energy spectrum, and the magnetic field strength. If these vary smoothly along the satellite trajectory,

no fundamental boundary is crossed when they reach a combination that makes the modulations negligible.

The fact that the amplitude of the flux oscillations is large at the sunward boundary suggests that the disturbances originate here and then propagate to other regions. In this context, some theoretical calculations by Smit [1968] are relevant. He has developed a fluid dynamical model which yields a resonance frequency for the piston-like motion of the nose of the magnetopause. The results are in good agreement with experimental observations.

Anderson et al. [1968] have found a longer periodicity, in addition to the periodicity of a few minutes. The profile of orbit 5 could be taken as evidence for the existence of a period of about 2.2 hours. Orbit 6 suggests a "relaxation time" of about 2 hours. Here is one example of fast-rise, slow-fall fluctuations, which is explained well by a fast expansion of the particle region followed by a slow contraction or relaxation. This example provides ground enough for speculating that one should, perhaps, seek to explain other fast-slow fluctuations, both here and elsewhere in the magnetosphere, by the sudden expansion of a region that already contains energetic particles followed by a slower contraction. This mechanism is to be

contrasted with the sudden injection of particles onto previously "empty" field lines, and with the sudden heating of the pre-existing plasma.

It has been shown that the so-called detached spikes seen here at the sunward boundary are detached only in the sense that they are separated in the time profiles from the main body of particles. Rosser [1963], Freeman [1964], and Konradi and Kaufmann [1965] have given the same interpretation of detached spikes. However, Frank and Van Allen [1964] and Fan et al. [1964 and 1965] suggest that the spikes they detect result from local acceleration of the transition region plasma. It is possible that both processes, local acceleration and boundary movements, occur. The results shown here and those of Konradi and Kaufmann [1965] demonstrate the great value of measurements of anisotropy in the spikes and simultaneous measurements of the local magnetic field. Such measurements should be able to distinguish between spikes that <u>can</u> be attributed to boundary movements and those that <u>cannot</u>.

Orbit 2 contains an example of a magnetopause crossing on the sunward side in which the energetic particle boundary does not coincide with the magnetopause as defined by the magnetic field. However, the particles beyond the boundary have a different character--they are streaming. We can only guess about their

origin. They could be particles that are leaking out from the magnetosphere.

C. Anisotropy

Roederer [1967] has calculated longitudinal drift paths for particles in an asymmetrical static model field and has shown how the drift depends on the equatorial pitch angle of the particles. One of his conclusions is that "equatorial pitch angles tend to align along the field lines on the night side of the magnetosphere and perpendicular to the field on the day side." The results shown here are in agreement with this prediction except for the two cases in which the pitch angle distribution apparently changed during the pass. In these cases, flux peaked at right angles to the field was seen on the night side. We offer no explanation for these exceptions, although they might be important observations. The simultaneous change in the rate of increase of the magnetic field is probably significant. It may also be relevant that the satellite was far from the equator at these times.

The strong anisotropy seen in the tail of particles on orbit 9 could be due to the same mechanism. If this is so, we must abandon the common assumption that particles in the distant magnetosphere (e.g., those seen on orbits 9 and 12) cannot make complete longitudinal drifts around the earth (see, for example,

Anderson [1965] and O'Brien [1967]). If their anisotropy is due to the process described by Roederer, complete longitudinal drift must take place. Of course, a more complex field model is needed to produce the required effect. The observations place certain limitations on the large scale field configuration in the outer magnetosphere; the field must be sufficiently regular, even in the distant parts, to keep the particles trapped while they drift in longitude.

An alternative explanation, at least for the tail of particles near the neutral sheet, is that they have been accelerated from the neutral sheet by a mechanism such as the one discussed by Piddington [1967]. See also Axford [1967]. In this theory, field lines, having recombined in the tail across the neutral sheet, contract toward the earth and accelerate the particles that are trapped in the bottle formed by the lines. The particles are accelerated by a Fermi process because of the approaching mirror points, and also by betatron acceleration caused by the increasing field strength. If the Fermi process is the more important (this is likely on orbit 9 since the measured field is still only a few gammas) then the pitch angles are decreased. Thus, the three gross characteristics seen on orbit 9 are produced; namely, <u>energetic</u> particles, mostly with <u>small</u> pitch angles, at the <u>earthward end</u> of the neutral sheet.

This theory, in contrast with the previous one, places no requirement on the large scale regularity of the field. However, it implies that the magnetospheric tail is an important source of particles for the radiation zones, whereas Roederer's theory says nothing about the source of the particles. The basic difference between the two theories is that the first uses a static field, whereas the second uses a time dependent field. We suggest that further tests of these theories should be made by trying to discern simultaneous temporal changes in the particle flux and the magnetic field.

V. SUMMARY

With the advantages of new trajectories through the magnetosphere and the ability to measure anisotropy, but with the disadvantage of a small total number of passes, we have attempted to map the distribution of energetic particle fluxes between about 5 and 20 R_E from the earth. We find that some of the terms used previously--core, skirt, cusp--are not very useful in describing the observations because of the definitions that they have been given. We find that most of the observations (including all the observations on the dusk side) point to the existence of a single central body of trapped particles whose boundary is everywhere oscillating. The shape of this inferred body is sketched in Figure 16. It occupies most of the region previously designated the core, the skirt, and the cusp. The oscillatory movements of the boundary are shown to be the cause of the "detached spikes" seen on the sunward side.

Some observations in the distant parts of the dawn side cannot be plausibly attributed to this body. We speculate, in view of the dawn-dusk asymmetries observed by others, that these fluxes are produced by a different (unknown) mechanism which is more effective on the dawn side than on the dusk side.

Measurements of the anisotropy, which is characteristic of the outer regions of the central body of particles, are mostly in qualitative agreement with the predictions made by Roederer [1967] from consideration of the longitudinal drift of particles in a static model field. Two exceptions were seen in which the pitch angle distribution appeared to change with time and/or position during the pass.

Anisotropic fluxes were seen at distances of up to about 16 R_E from the earth. If the anisotropy results from the mechanism described by Roederer, then the particles in those distant regions must, contrary to common belief, be able to drift in longitude completely around the earth. Alternatively, these anisotropic fluxes, especially those near the neutral sheet, could be construed as evidence for the acceleration of particles from the tail by field lines contracting toward the earth from the tail, i.e., evidence for the importance of non-static magnetic fields.

ACKNOWLEDGMENTS

The author is grateful to Professor J. A. Van Allen who designed the Explorer 33 experiment and has made available the full body of reduced particle observations for this study, and to Drs. D. S. Colburn and C. P. Sonett of the Ames Research Center of NASA for permission to use portions of their simultaneous magnetic field data before publication.

This work was supported by NASA Grant ~~NsG-233~~ NGR-16-001-002 and GSFC/NASA Contract NAS 5-9076, both with the University of Iowa.

REFERENCES

Anderson, K. A., "Energetic electron fluxes in the tail of the geomagnetic field," J. Geophys. Res. 70, 4741-4763 (1965).

Anderson, K. A., J. H. Binsack, and D. H. Fairfield, "Hydromagnetic disturbances of 3 to 15 minute period on the magnetopause and their relation to bow shock spikes," preprint (1968).

Anderson, K. A., H. K. Harris, and R. J. Paoli, "Energetic electron fluxes in and beyond the earth's outer magnetosphere," J. Geophys. Res. 70, 1039-1050 (1965).

Anderson, K. A. and N. F. Ness, "Correlation of magnetic fields and energetic electrons on the IMP 1 satellite," J. Geophys. Res. 71, 3705-3727 (1966).

Axford, W. I., "The interaction between the solar wind and the magnetosphere," Aurora and Airglow (Reinhold, 1967), pp. 499-509.

Bame, S. J., J. R. Asbridge, H. E. Felthauser, E. W. Hones, and I. B. Strong, "Characteristics of the plasma sheet in the earth's magnetotail," J. Geophys. Res. 72, 113-129 (1967).

Fan, C. Y., G. Gloeckler, and J. A. Simpson, "Evidence for > 30 keV electrons accelerated in the shock transition region beyond the earth's magnetospheric boundary," Phys. Rev. Letters 13, 149-153 (1964).

Fan, C. Y., G. Gloeckler, and J. A. Simpson, "Acceleration of particles in the earth's shock transition region and beyond," Proc. Int. Conf. Cosmic Rays, The Institute of Physics and the Physical Society, London, 1965, p. 105-108.

Frank, L. A., "A survey of electrons E > 40 keV beyond 5 earth radii with Explorer 14," J. Geophys. Res. 70, 1593-1626 (1965).

Frank, L. A. and J. A. Van Allen, "Measurements of energetic electonrs in the vicinity of the sunward magnetospheric boundary with Explorer 14," J. Geophys. Res. 69, 4923-4932 (1964).

Freeman, J. W., "The morphology of the electron distribution in the outer radiation zone and near the magnetospheric boundary as observed by Explorer 12," J. Geophys. Res. 69, 1691-1723 (1964).

Freeman, J. W., J. A. Van Allen, and L. J. Cahill, "Explorer 12 observations of the magnetospheric boundary and associated solar plasma on September 13, 1961," J. Geophys. Res. 68, 2121-2130 (1963).

Heppner, J. P., M. Sugiura, T. L. Skillman, B. G. Ledley, and M. Campbell, "OGO-A magnetic field observations," J. Geophys. Res. 72, 5417-5471 (1967).

Hills, H. K., "Observations of energetic electron intensities in the earth's outer radiation zone with OGO-1," University of Iowa Research Report 67-72 (1967).

Judge, D. L. and P. J. Coleman, "Observations of low-frequency hydromagnetic waves in the distant geomagnetic field: Explorer 6," J. Geophys. Res. 67, 5071-5090 (1962).

Konradi, A. and R. L. Kaufmann, "Evidence for rapid motion of the outer boundary of the magnetosphere," J. Geophys. Res. 70, 1627-1637 (1965).

Lin, R. P. and K. A. Anderson, "Periodic modulations of the energetic electron fluxes in the distant radiation zone," J. Geophys. Res. 71, 1827-1835 (1966).

Montgomery, M. D., "Observations of electrons in the earth's magnetotail by Vela launch 2 satellites," J. Geophys. Res. 73, 871-889 (1968).

O'Brien, B. J., "Interrelations of energetic charged particles in the magnetosphere," Solar-Terrestrial Physics (Academic Press, 1967), p. 169-211.

Piddington, J. H., "A theory of auroras and the ring current," J. Atmos. and Terrest. Phys. 29, 87-105 (1967).

Roederer, J. G., "On the adiabatic motion of energetic particles in a model magnetosphere," J. Geophys. Res. 72, 981-992 (1967).

Rosser, W. G. V., "Changes in the structure of the outer radiation zone associated with the magnetic storm of September 30, 1961," J. Geophys. Res. 68, 3131-3148 (1963).

Rothwell, P., "Energetic particle observations from IMP-B satellite," Space Sci. Rev. 7, 278-287 (1967).

Serlemitsos, P., "Low energy electrons in the dark magnetosphere," J. Geophys. Res. 71, 61-77 (1966).

Smit, G. R., "On the oscillatory motion of the nose region of the magnetopause," preprint (1968).

Van Allen, J. A. and N. F. Ness, "Observed particle effects of an interplanetary shock wave on July 8, 1966," J. Geophys. Res. 72, 935-942 (1967).

FIGURE CAPTIONS

Figure 1 Relevant portions of the first 17 orbits of Explorer 33 in two projections in geocentric solar ecliptic coordinates. The orbits are numbered chronologically, with the encircled number at the beginning of each pass. The diamond symbols appear also on the time profiles in Figure 3.

Figure 2 The angular acceptance of the collimators and the sectoring scheme.
(a) In a plane through the spin axis.
(b) In the plane perpendicular to the spin axis.
The acceptance quoted here is defined by the angle from the axis of the collimator at which the counting efficiency is 10% of its maximum value.

Figure 3 The time profiles GA, GB, and GC in counts per second are shown as functions of universal time (day : hour). January 1 is day 0. Geomagnetic latitude, λ_m, in degrees is shown every three hours. The diamond symbols enable the fluxes to be located in Figure 1. The 24-hour sum of the K_p indices for the period of each plot is marked in the top right hand corner.

Figure 4 Orbit 12 in geomagnetic coordinates, ignoring longitude. The flux boundaries from orbits 13, 14, and 15 are shown.

Figure 5 Comparison of the approximate direction of maximum flux, α, with the direction of the magnetic field, both measured in the plane perpendicular to the satellite's spin axis. $\alpha = 85° \pm \tan^{-1}(GA/GB)$. α and the field direction were calculated for every tenth sequence, except during orbit 5 when they were calculated for every fiftieth sequence.

Figure 6 The same as Figure 5 for the two cases in which the relationship between α and the field direction changed during the pass.

Figure 7 Showing the abrupt changes in the rate of increase of field magnitude. The arrows mark sequences that fall between the first two joined points in Figure 6.

Figure 8 Oscillations and "detached spikes" near the sunward boundary on orbit 9. Solar magnetospheric X, Y, and Z axes are in the directions: $\Phi = 0$, $\Phi = 90$, and $\theta = +90$, respectively.

Figure 9 Oscillations and "detached spikes" near the sunward boundary on orbit 2.

Figure 10 The sunward boundary on orbit 12.

Figure 11 Projection of portions of orbit 9 and 16 onto the solar ecliptic X-Z plane. The dashed lines show the intersection of the geomagnetic equatorial plane with the X-Z plane at the times corresponding to the crosses marked on the orbits, and the positions of presumed neutral sheets parallel to the X axis and passing through the crosses.

Figure 12 The neutral sheet crossing on orbit 16.

Figure 13 The "expanded neutral sheet" crossing on orbit 9.

Figure 14 Suggested location of orbits in magnetic frame of reference.

Figure 15 The same as Figure 5 for the four regions encountered on orbit 9.

Figure 16 A rough sketch of the shape of the central body of trapped particles inferred from the present measurements showing, qualitatively, the change of meridional cross section with longitude. For simplicity, the geomagnetic equatorial plane is made to coincide with the ecliptic plane.

Explorer 33 trajectory and reference points

Solar ecliptic co-ordinates

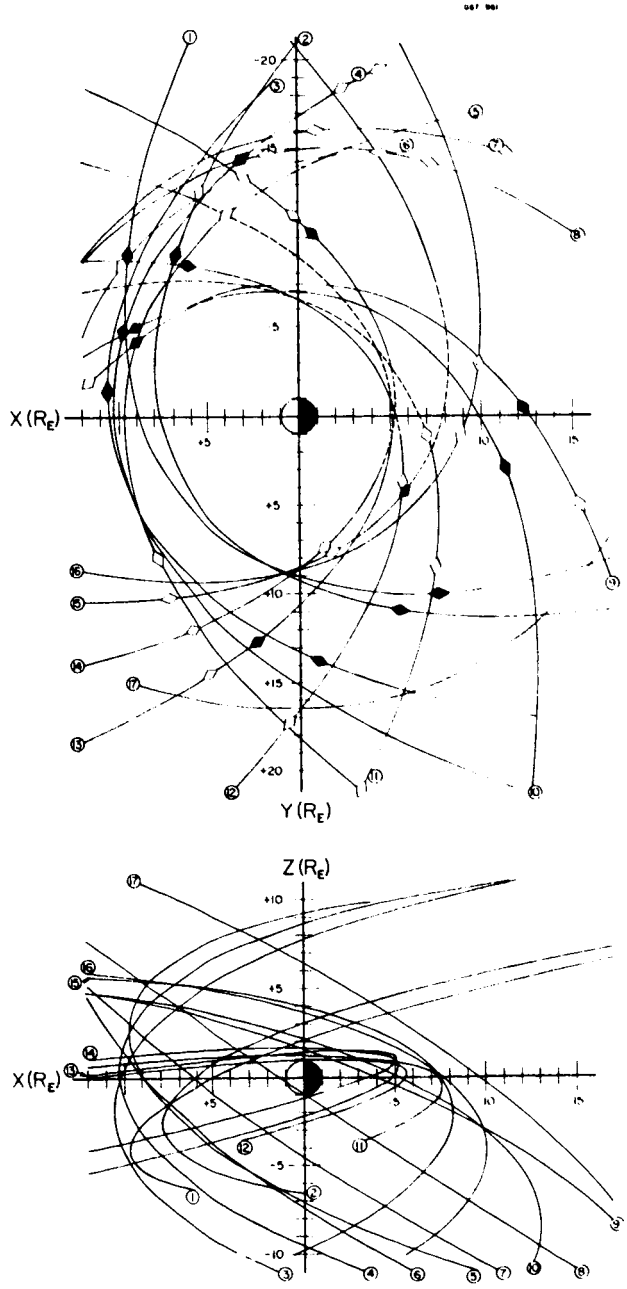

Figure 1

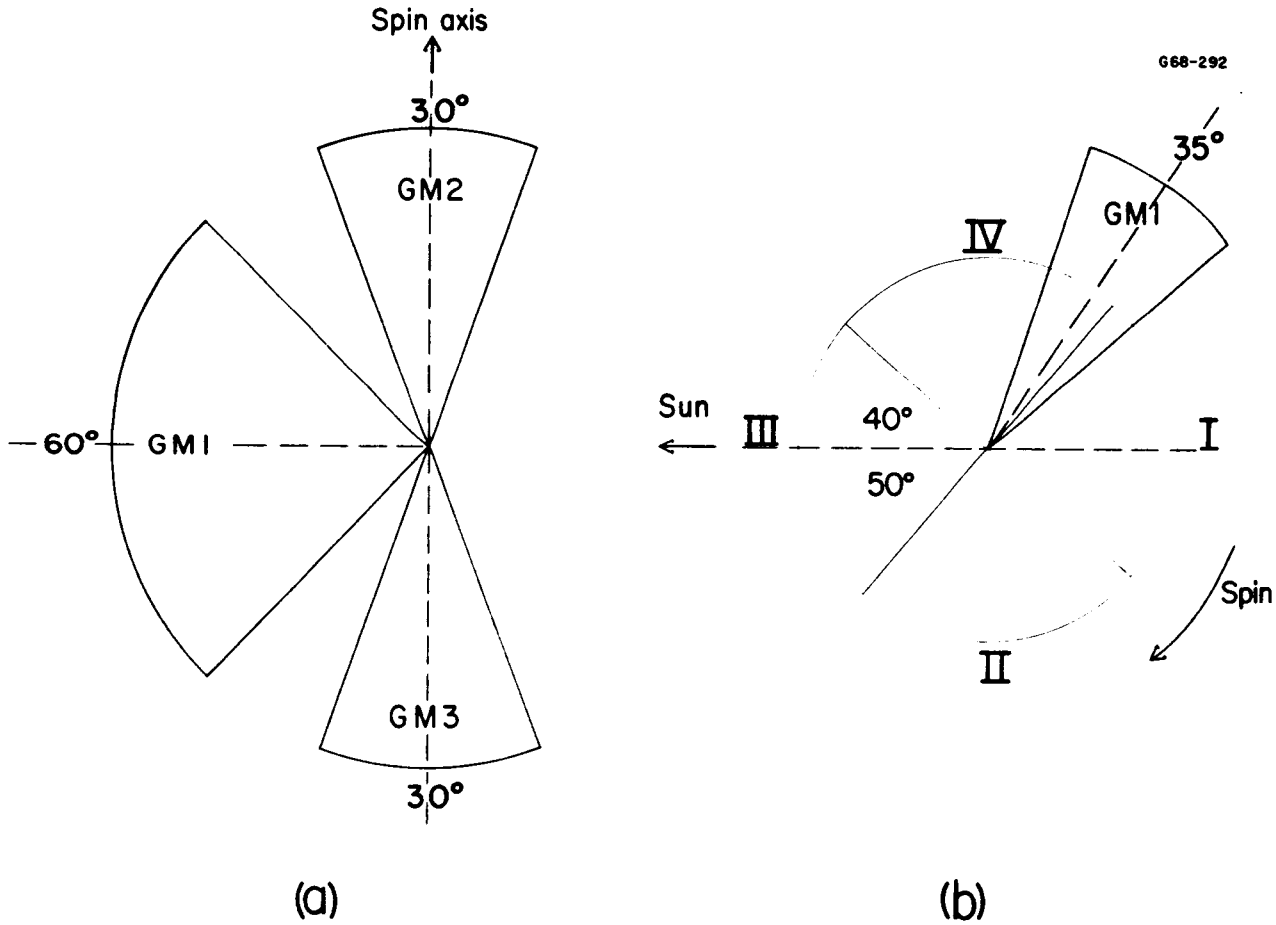
Spin axis
30°
GM2
60°
GM1
GM3
30°
(a)
G68-292
35°
GM1
IV
Sun
III
40°
I
50°
Spin
II
(b)

Figure 2

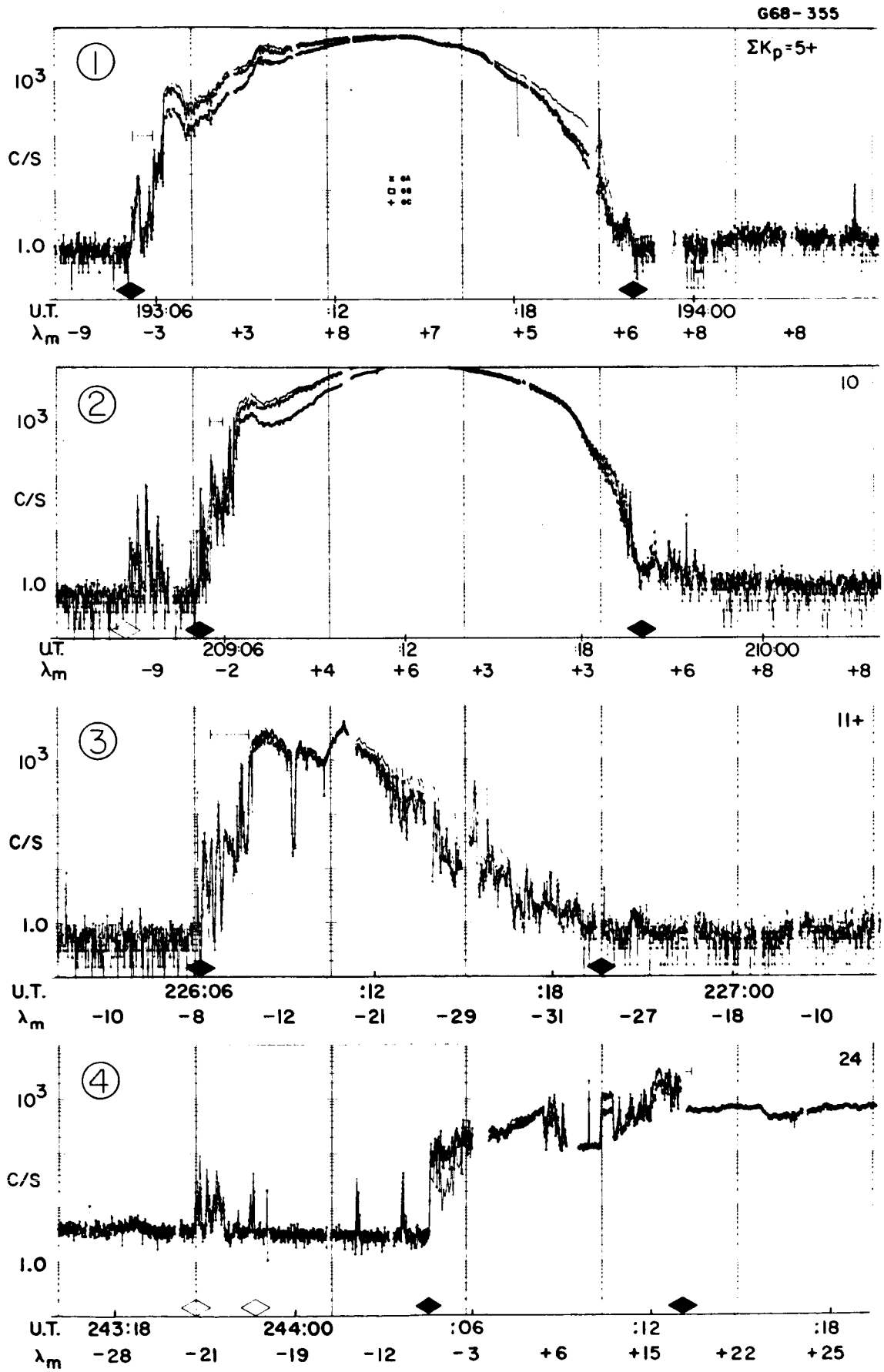
G68-355
ΣKp=5+
10³
C/S
1.0
①
U.T. 193:06 :12 :18 194:00
λm -9 -3 +3 +8 +7 +5 +6 +8 +8
10
②
209:06 :12 :18 210:00
-9 -2 +4 +6 +3 +3 +6 +8 +8
11+
③
226:06 :12 :18 227:00
-10 -8 -12 -21 -29 -31 -27 -18 -10
24
④
243:18 244:00 :06 :12 :18
-28 -21 -19 -12 -3 +6 +15 +22 +25

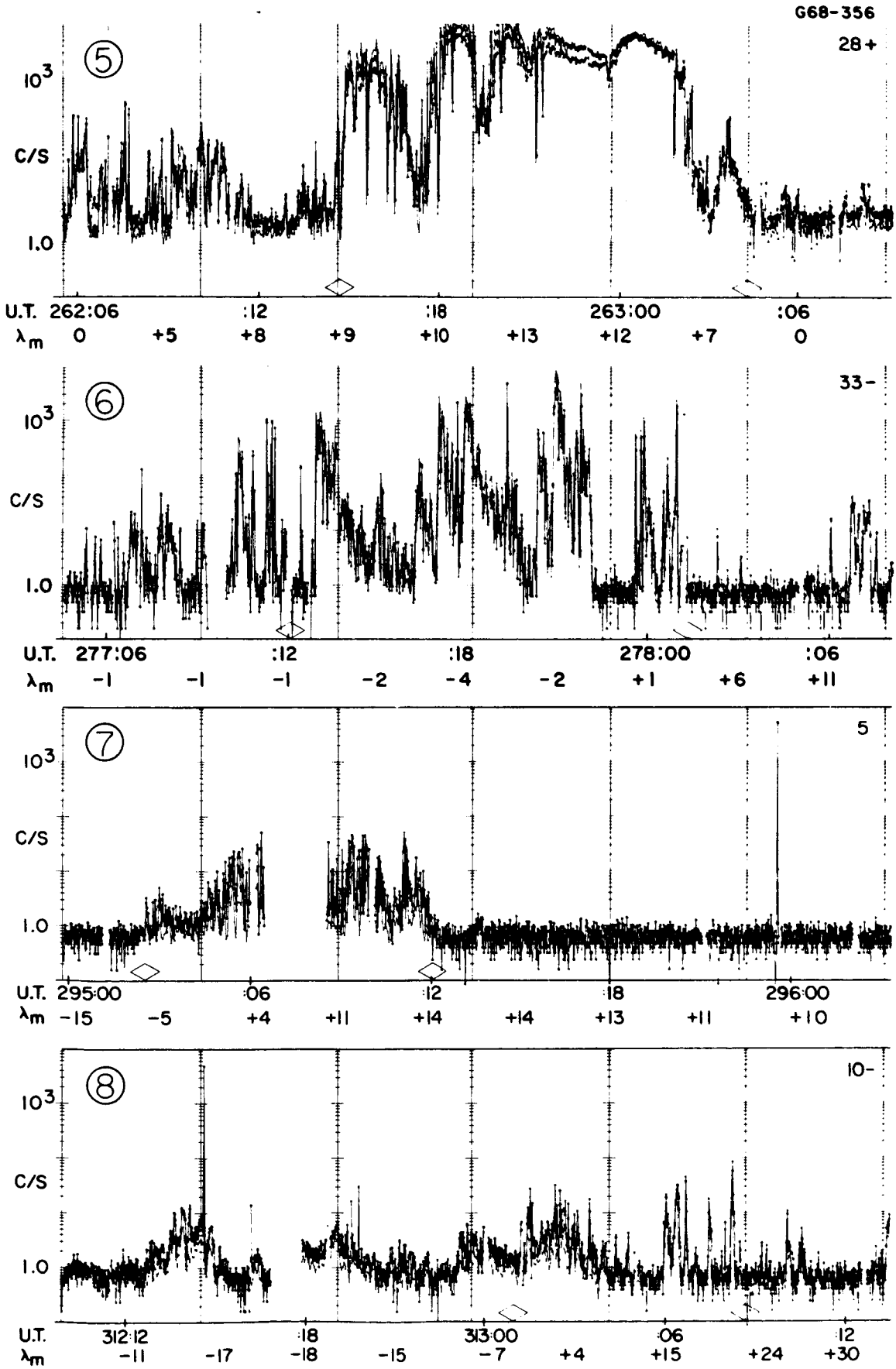
G68-356
28+
⑤
10^3
C/S
1.0
U.T. 262:06 :12 :18 263:00 :06
λ_m 0 +5 +8 +9 +10 +13 +12 +7 0
33-
⑥
10^3
C/S
1.0
U.T. 277:06 :12 :18 278:00 :06
λ_m -1 -1 -1 -2 -4 -2 +1 +6 +11
5
⑦
10^3
C/S
1.0
U.T. 295:00 :06 :12 :18 296:00
λ_m -15 -5 +4 +11 +14 +14 +13 +11 +10
10-
⑧
10^3
C/S
1.0
U.T. 312:12 :18 313:00 :06 :12
λ_m -11 -17 -18 -15 -7 +4 +15 +24 +30

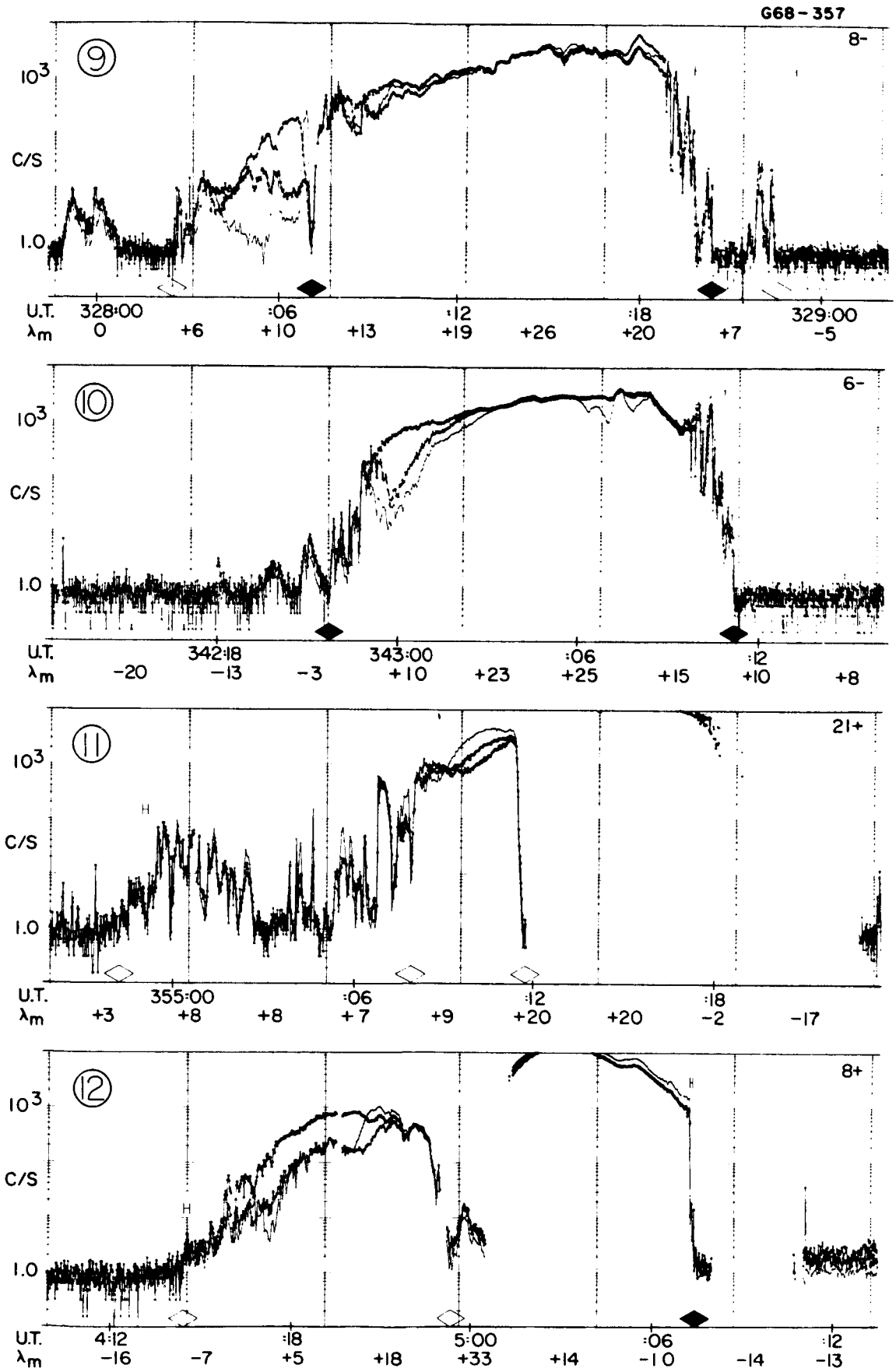
G68-357
8-
⑨
10³
C/S
1.0
U.T. 328:00 :06 :12 :18 329:00
λm 0 +6 +10 +13 +19 +26 +20 +7 -5
6-
⑩
10³
C/S
1.0
U.T. 342:18 343:00 :06 :12
λm -20 -13 -3 +10 +23 +25 +15 +10 +8
21+
⑪
H
10³
C/S
1.0
U.T. 355:00 :06 :12 :18
λm +3 +8 +8 +7 +9 +20 +20 -2 -17
8+
⑫
H
H
10³
C/S
1.0
U.T. 4:12 :18 5:00 :06 :12
λm -16 -7 +5 +18 +33 +14 -10 -14 -13

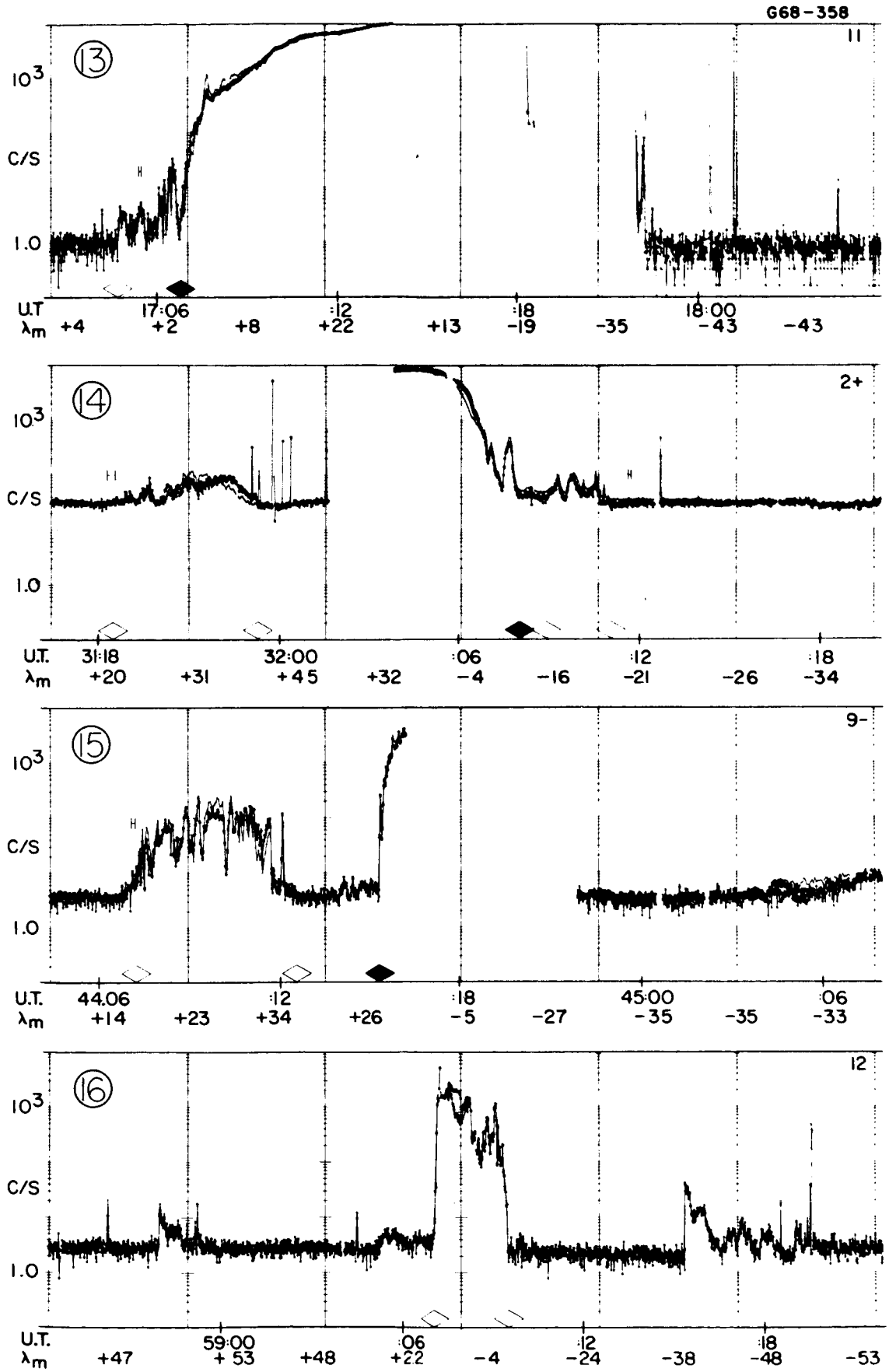
G68-358
11
13
10^3
C/S
1.0
U.T
λ_m +4
17:06
+2
+8
:12
+22
+13
:18
-19
-35
18:00
-43
-43
2+
14
10^3
C/S
1.0
U.T.
λ_m +20
31:18
+31
32:00
+45
+32
:06
-4
-16
:12
-21
-26
:18
-34
9-
15
10^3
C/S
1.0
U.T.
λ_m +14
44.06
+23
:12
+34
+26
:18
-5
-27
45:00
-35
-35
06
-33
12
16
10^3
C/S
1.0
U.T.
λ_m +47
59:00
+53
+48
:06
+22
-4
:12
-24
-38
:18
-48
-53

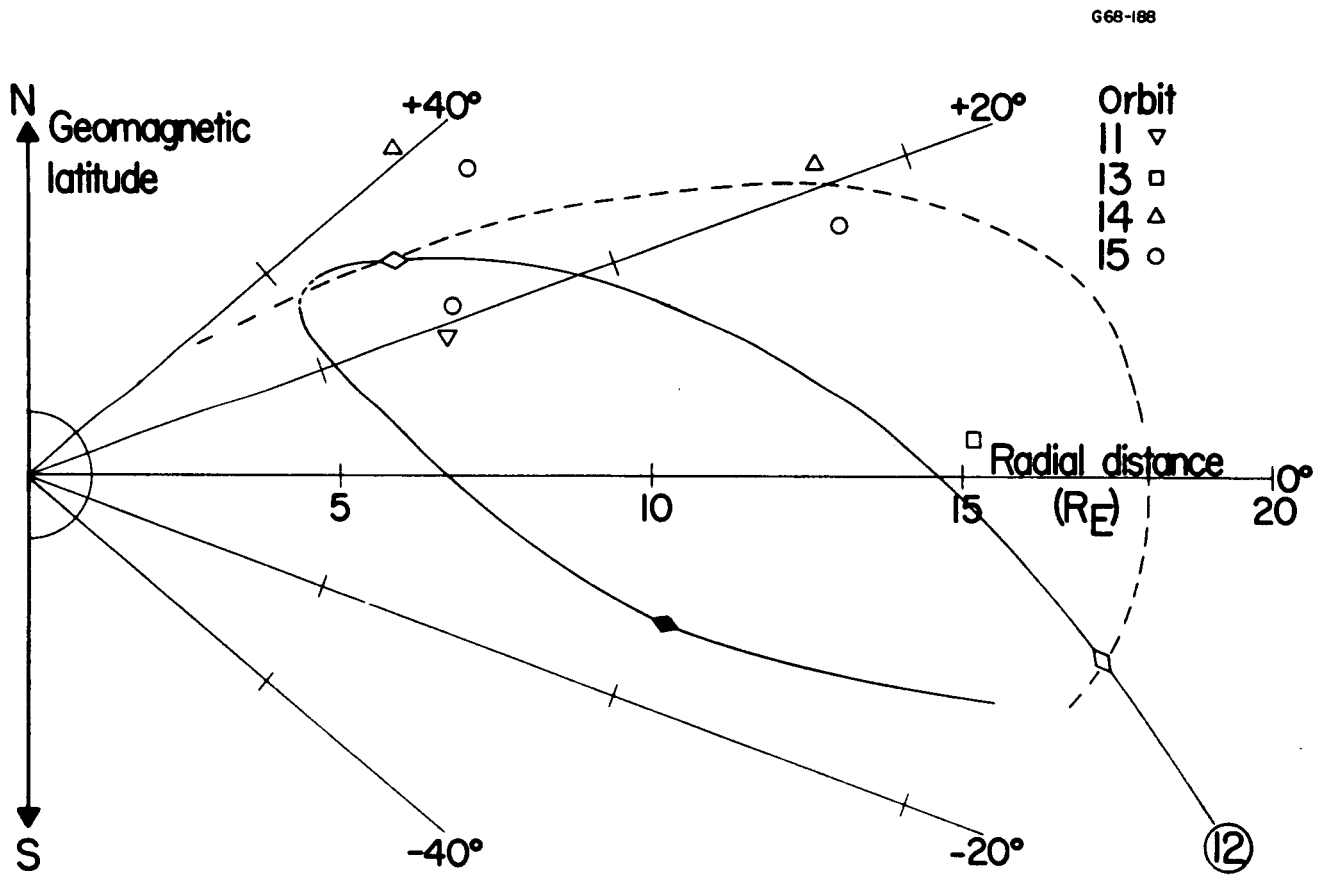
G68-188
N
Geomagnetic
latitude
+40°
+20°
Orbit
11
13
14
15
Radial distance
(RE)
5
10
15
20
0°
S
-40°
-20°
12

Figure 4

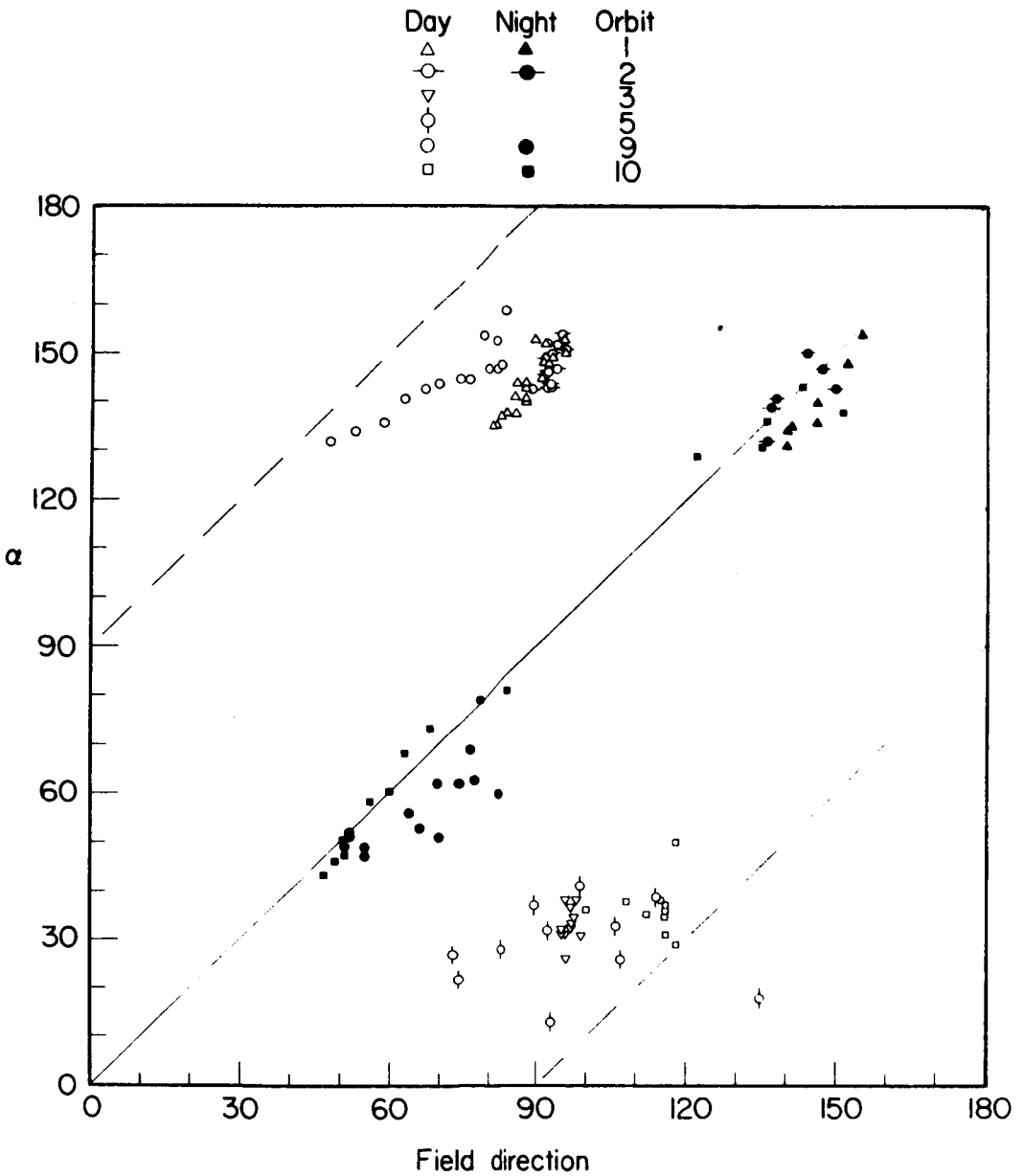
G68-75
Day
Night
Orbit
1
2
3
5
9
10
180
150
120
90
60
30
0
α
0
30
60
90
120
150
180
Field direction

Figure 5

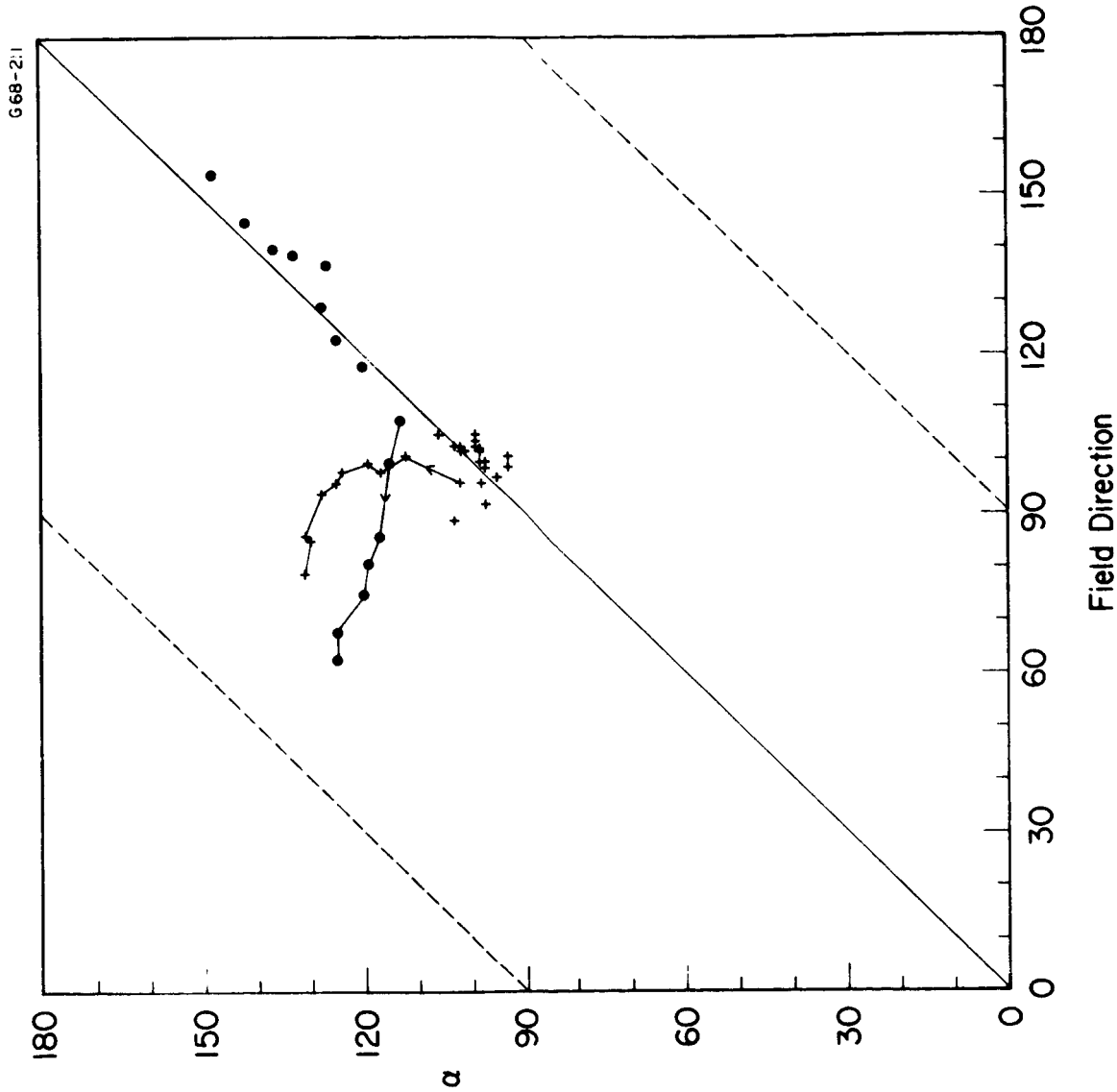
G68-211
180
150
120
90
60
30
0
α
0
30
60
90
120
150
180
Field Direction

Figure 6

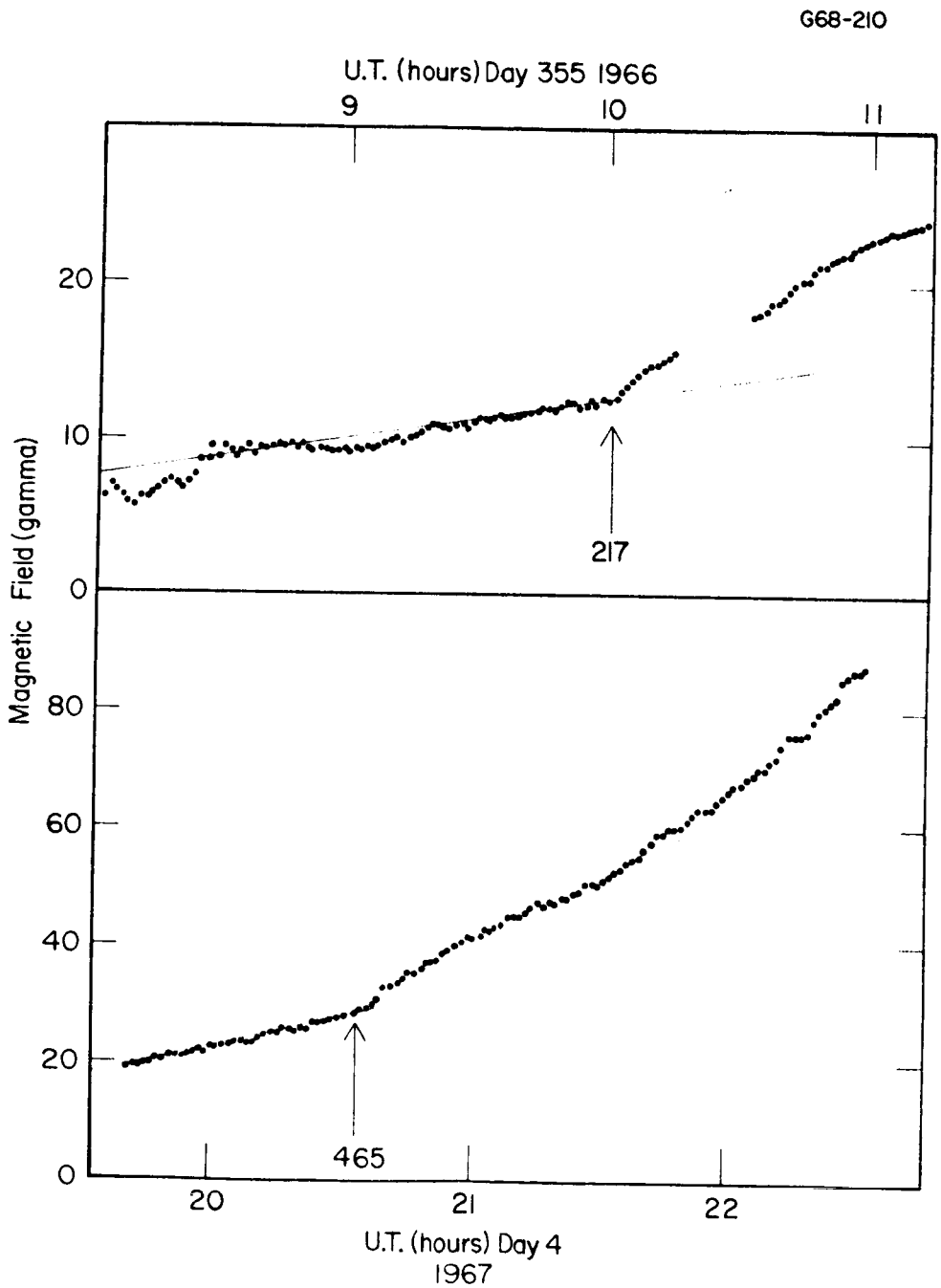
G68-210
U.T. (hours) Day 355 1966
9
10
11
20
10
0
217
Magnetic Field (gamma)
80
60
40
20
0
465
20
21
22
U.T. (hours) Day 4
1967

Figure 7

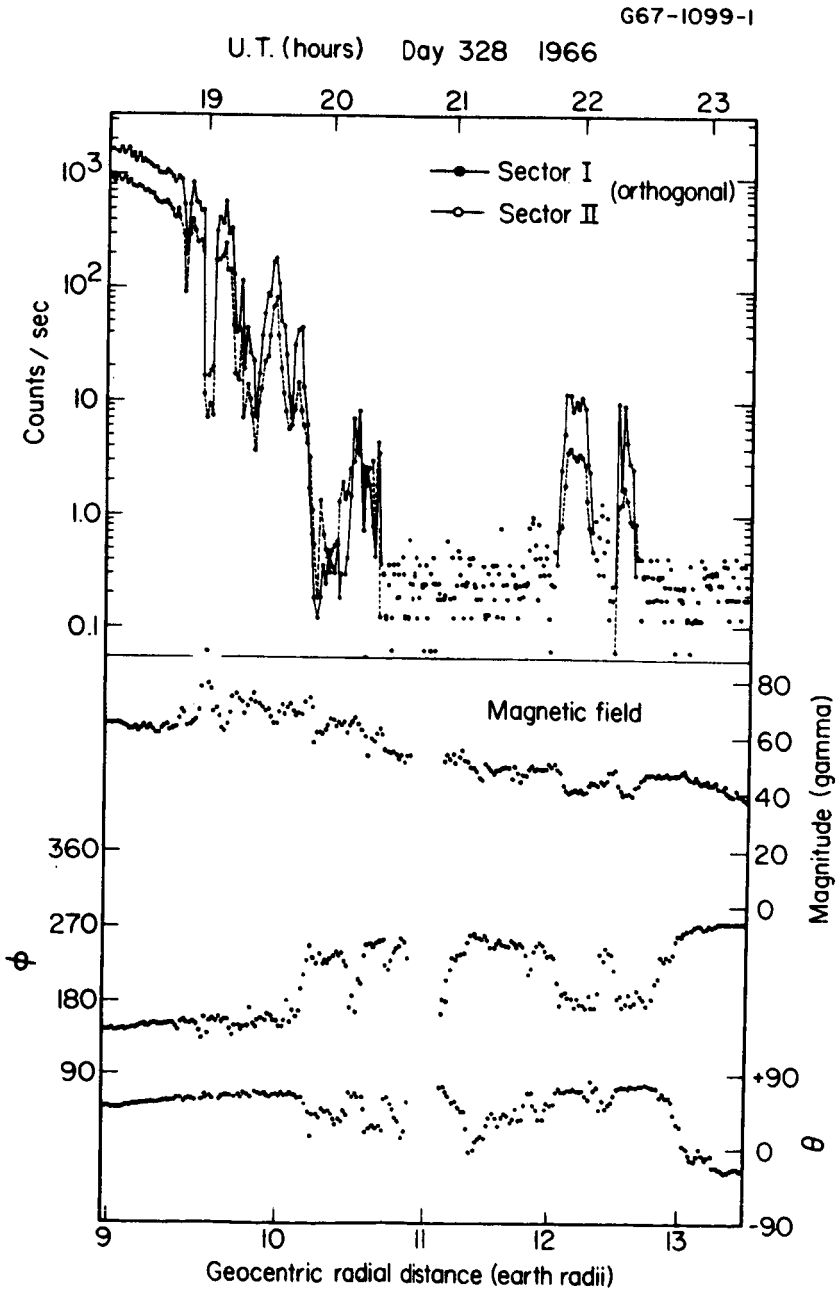
G67-1099-1
U.T. (hours) Day 328 1966
19
20
21
22
23
Sector I
Sector II
(orthogonal)
Counts / sec
10^3
10^2
10
1.0
0.1
Magnetic field
80
60
40
20
0
Magnitude (gamma)
360
270
180
90
ϕ
+90
0
-90
θ
9
10
11
12
13
Geocentric radial distance (earth radii)

Figure 8

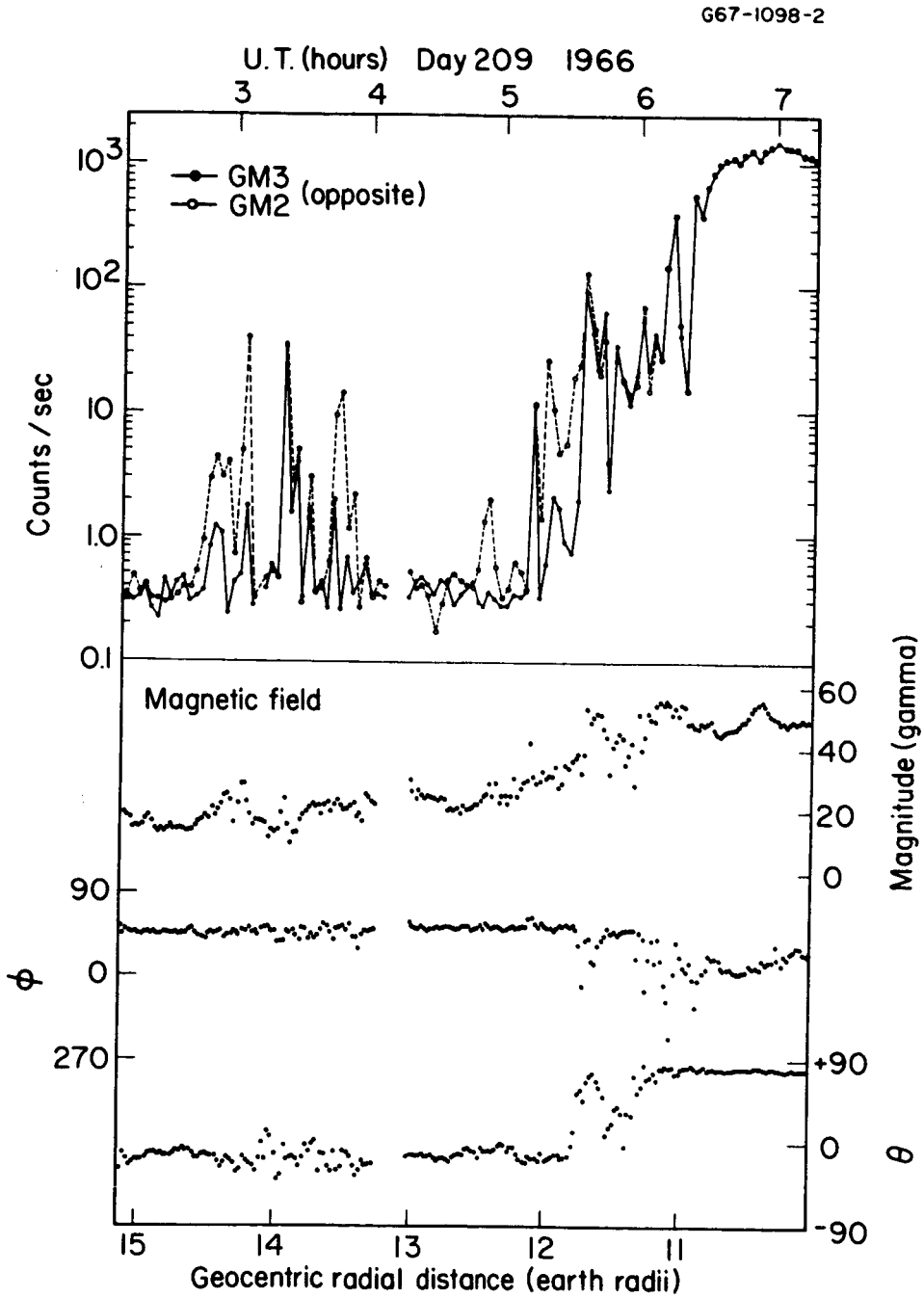
G67-1098-2
U.T. (hours) Day 209 1966
3
4
5
6
7
GM3
GM2 (opposite)
Counts / sec
Magnetic field
Magnitude (gamma)
60
40
20
0
90
0
270
+90
0
-90
θ
15
14
13
12
11
Geocentric radial distance (earth radii)

Figure 9

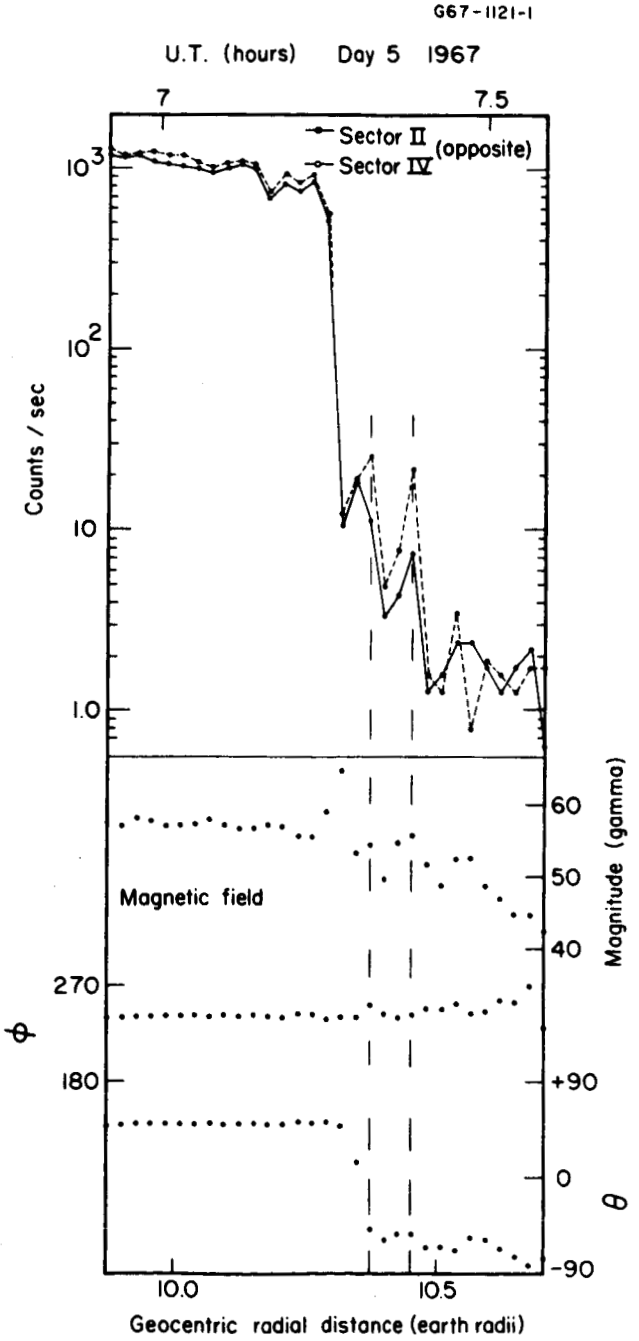
G67-1121-1
U.T. (hours) Day 5 1967
7
7.5
Sector II
Sector IV (opposite)
10^3
10^2
10
1.0
Counts / sec
Magnetic field
60
50
40
Magnitude (gamma)
270
180
ϕ
+90
0
-90
θ
10.0
10.5
Geocentric radial distance (earth radii)

Figure 10

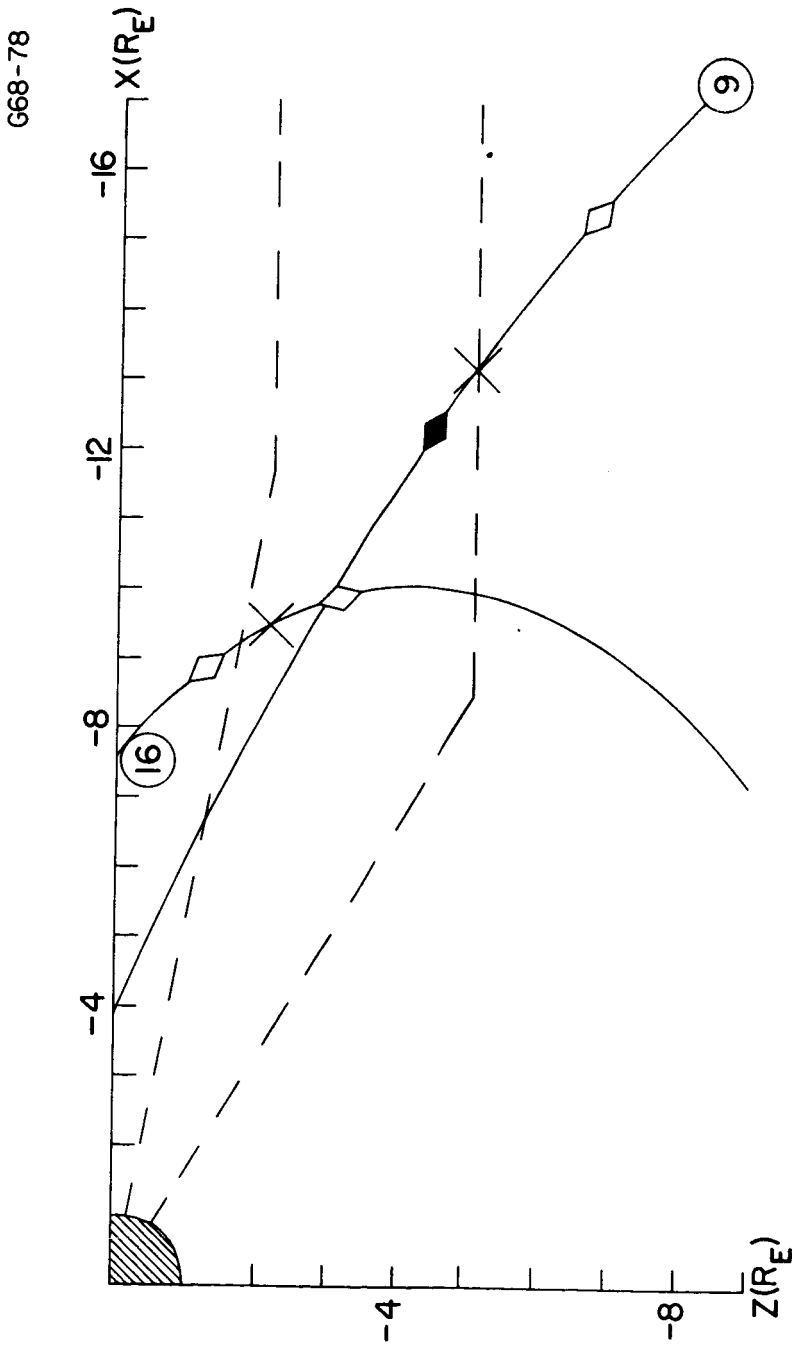

Figure 11

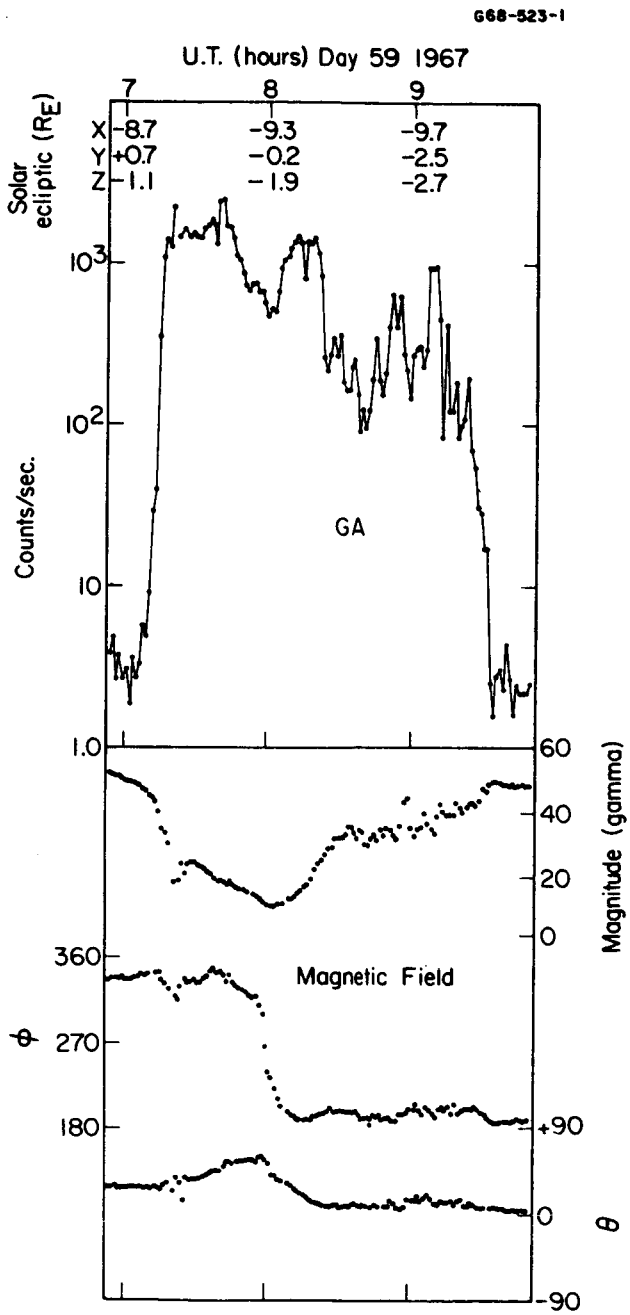
G68-523-1
U.T. (hours) Day 59 1967
7
8
9
Solar ecliptic (R_E)
X -8.7 -9.3 -9.7
Y +0.7 -0.2 -2.5
Z -1.1 -1.9 -2.7
10^3
10^2
10
1.0
Counts/sec.
GA
60
40
20
0
Magnitude (gamma)
360
270
180
θ
Magnetic Field
+90
0
-90
θ

Figure 12

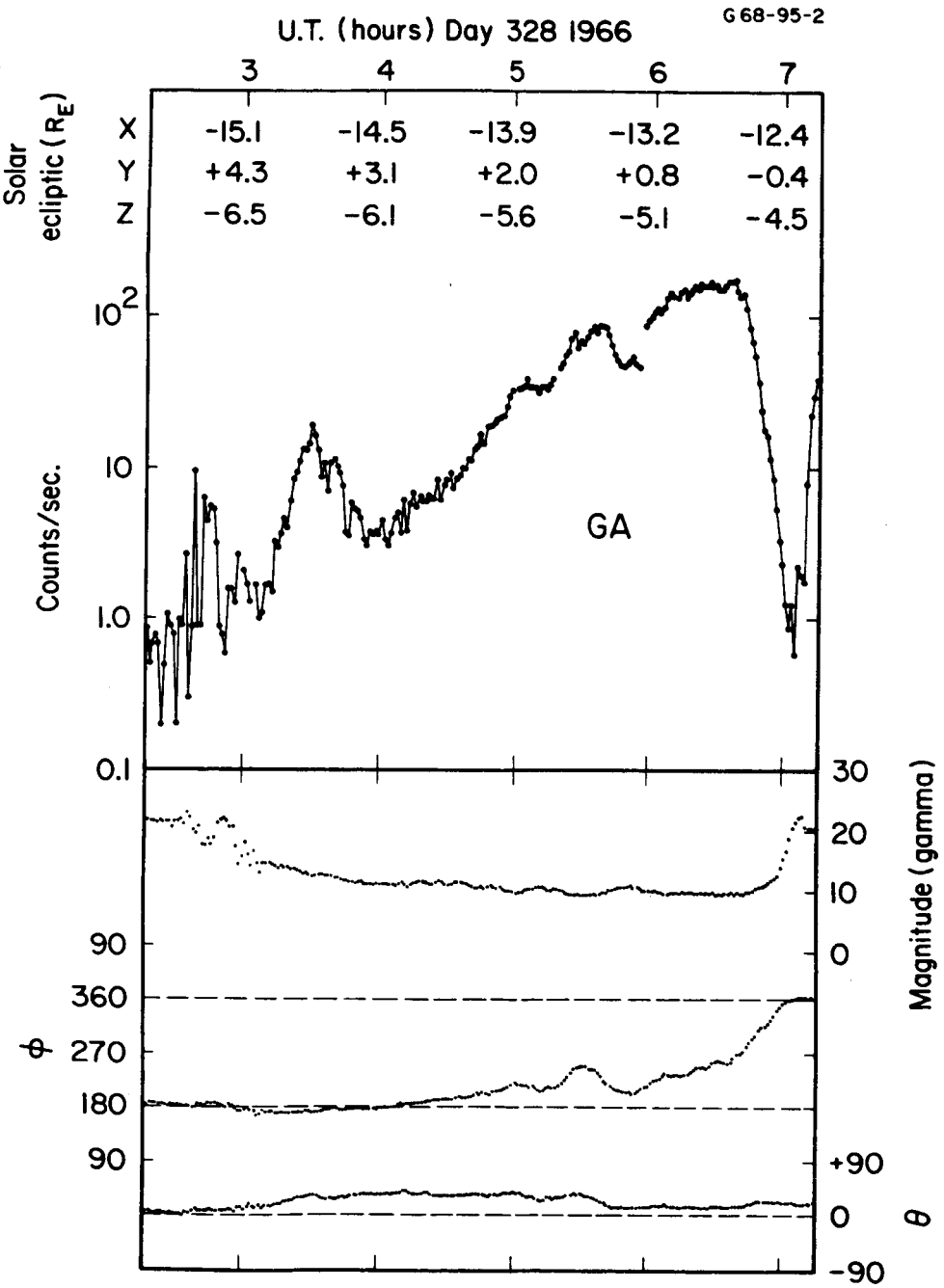
U.T. (hours) Day 328 1966
G68-95-2
3
4
5
6
7
Solar ecliptic (R_E)
X -15.1 -14.5 -13.9 -13.2 -12.4
Y +4.3 +3.1 +2.0 +0.8 -0.4
Z -6.5 -6.1 -5.6 -5.1 -4.5
10^2
10
1.0
0.1
Counts/sec.
GA
30
20
10
0
Magnitude (gamma)
90
360
θ 270
180
90
+90
0
-90
θ

Figure 13

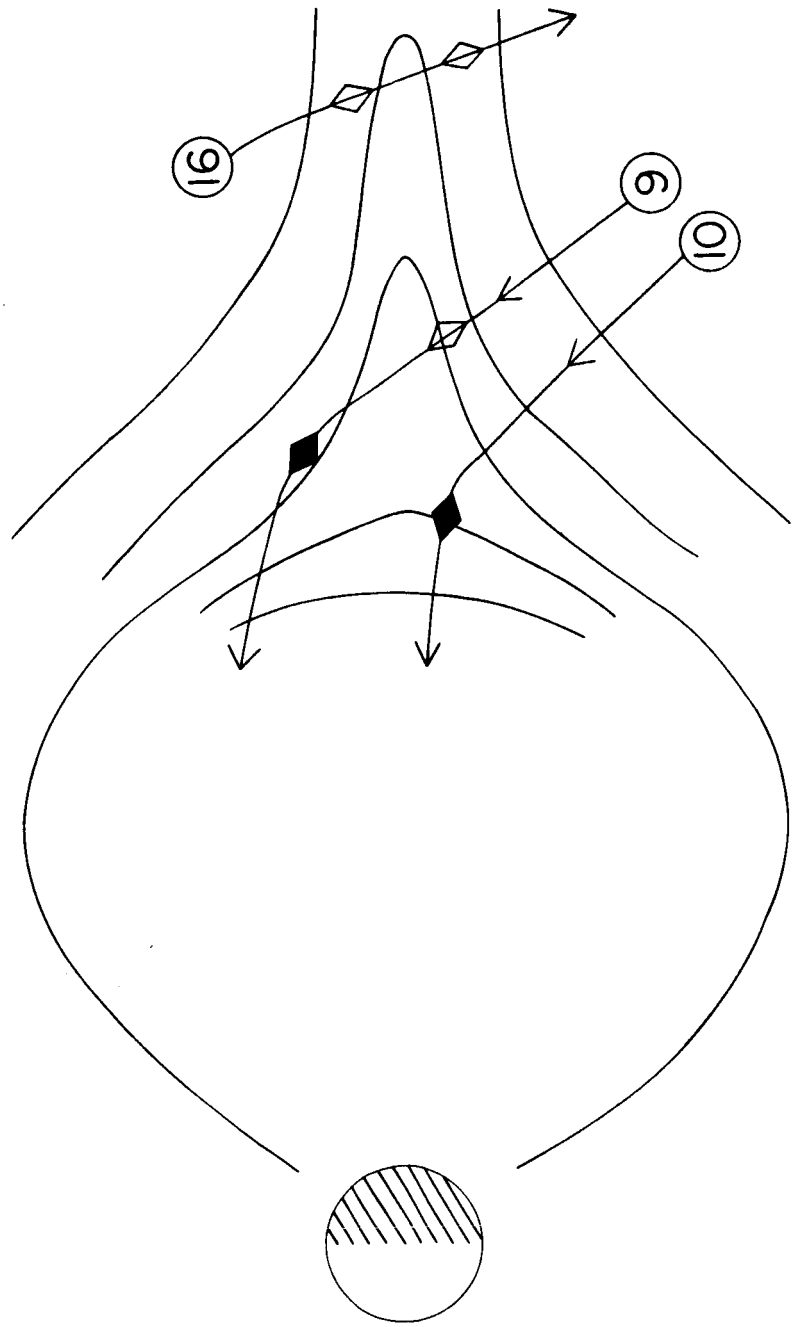

Figure 14

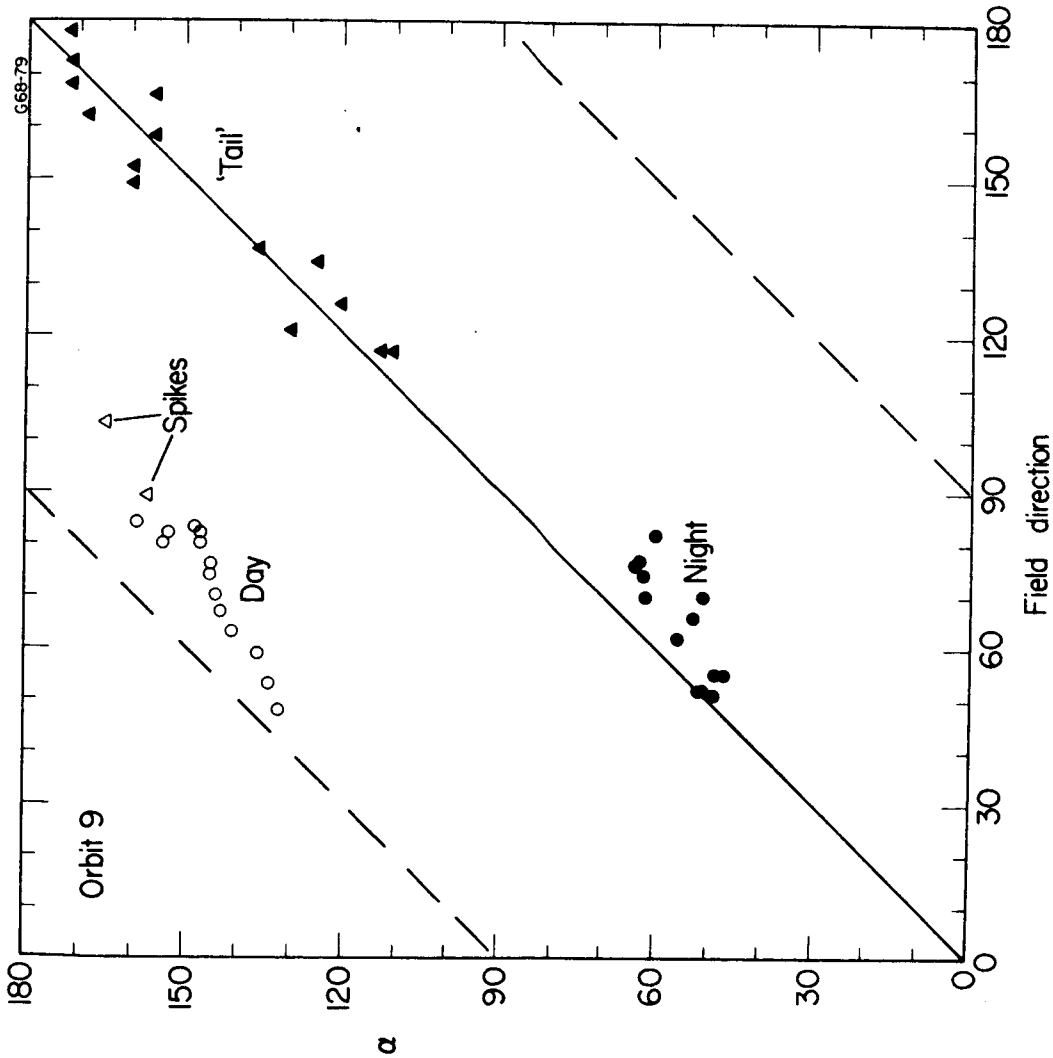
668-79
Orbit 9
'Tail'
Spikes
Day
Night
α
Field direction
0
30
60
90
120
150
180

Figure 15

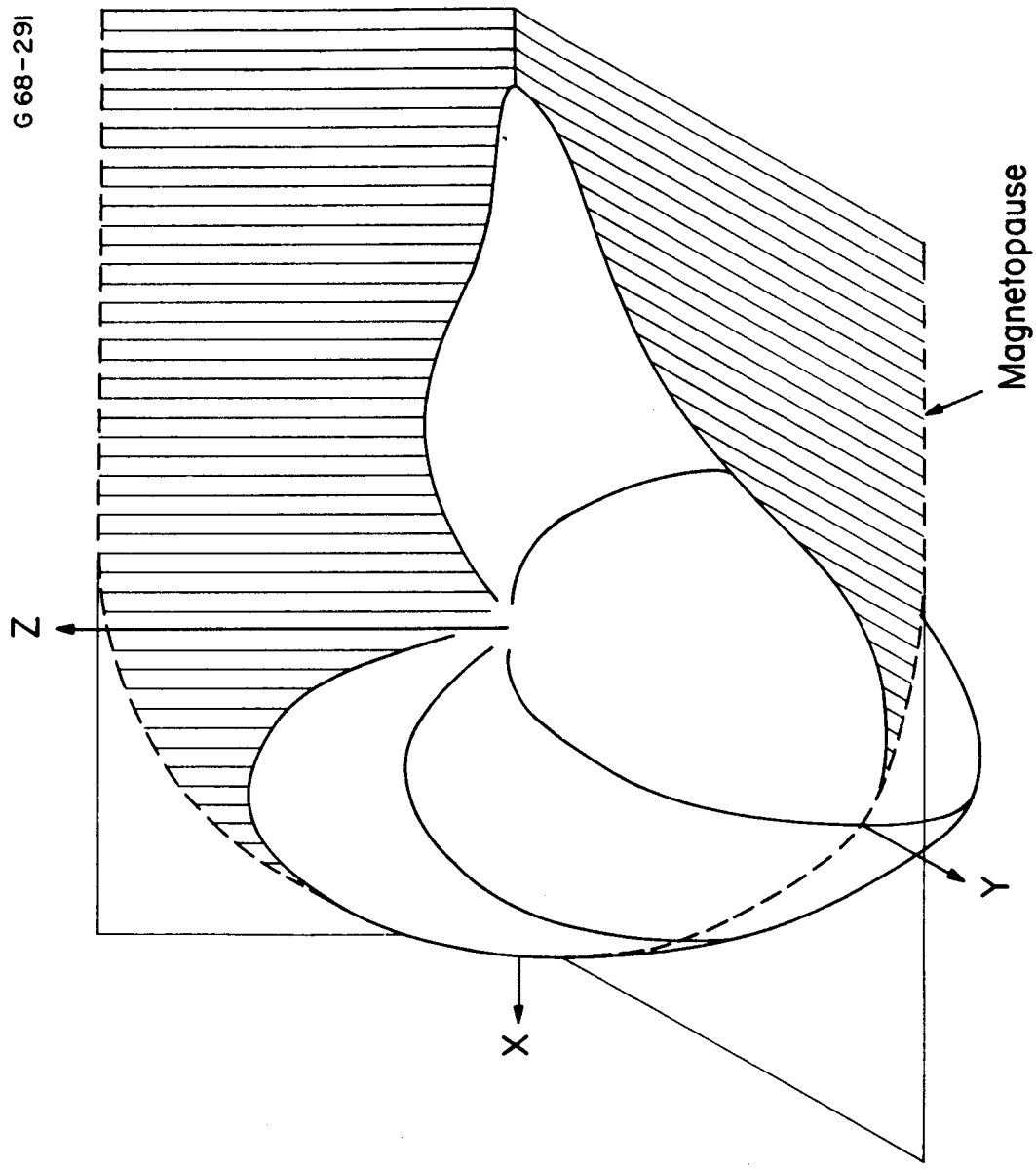

Figure 16